Functional and Energetic Characterization of P-gp Mediated Doxorubicin Transport in Rainbow Trout (*Oncorhynchus mykiss*) Hepatocytes

by

Jennifer Lee Hildebrand
B.Sc., Simon Fraser University, 2004

PROJECT SUBMITTED IN PARTIAL FULFILLMENT OF
THE REQUIREMENTS FOR THE DEGREE OF

MASTER OF ENVIRONMENTAL TOXICOLOGY

In the
Department of Biological Sciences

SIMON FRASER UNIVERSITY

Spring 2008

APPROVAL

Name: Jennifer Lee Hildebrand

Degree: Master of Environmental Toxicology

Title of Thesis: Functional and energetic characterization of P-gp mediated doxorubicin transport in rainbow trout (*Oncorhynchus mykiss*) hepatocytes

Examining Committee:

Chair: Dr. A. Kermode, Professor

Dr. C. J. Kennedy, Professor
Department of Biological Sciences, SFU

Dr. R. A. Nicholson, Associate Professor
Department of Biological Sciences, SFU

Dr. R. C. P. Law, Professor
Department of Biological Sciences

Public Examiner

Date Defended: February 12, 2008

ABSTRACT

ATP-dependent, P-glycoprotein-mediated efflux of xenobiotics is an important cellular defense strategy, preventing intracellular accumulation. Studies have shown that costs associated with cellular defense may be substantial however, few studies have examined the costs associated with P-gp transport. Therefore, the activity and energetic costs associated with P-gp transport of doxorubicin were examined in trout hepatocytes. Accumulation and efflux of doxorubicin was concentration dependent, and tariquidar significantly inhibited efflux by 57%, 61%, and 50% in the 125, 75, and 25 μM groups compared to tariquidar un-treated groups. P-gp efflux of doxorubicin significantly reduced intracellular ATP concentration, adenylate energy charge, and phosphorylation potential with highest percent decreases of 25%, 11%, and 53% respectively, and increased concentrations of ADP, AMP, and Pi with highest percent increases of 26%, 36%, and 11% respectively compared to controls and tariquidar-treated groups. These results indicate that exposure of hepatocytes to DOX caused an increase in P-gp activity which was shown to affect cellular energetics.

Keywords: P-glycoprotein; doxorubicin; tariquidar; adenylate energy charge, phosphorylation potential; rainbow trout; energetic costs

Subject Terms: Toxicology; p-glycoprotein; bioenergetics; adenylate energy charge

DEDICATION

This work is dedicated to my family, especially my parents who have always stood by me and given me the motivation to accomplish my goals.

ACKNOWLEDGEMENTS

I would like to thank Dr. C.J. Kennedy and Dr. R.A. Nicholson for their advice, support, and involvement in this project. I would especially like to thank Dr. C.J. Kennedy for giving me the opportunity to work in his lab and for being a mentor throughout my year's at Simon Fraser University. I would also like to thank the staff of the biology department, especially the lab technicians who have assisted me many times over the past few years. Onkar Bains and Denny Lee are thanked for the assistance with the project, and Dr. Susan Bates, Rob Robey and David Norris are thanked for XR9576. Lastly I would like to thank my family and friends for their support, advice, and many needed laughs.

TABLE OF CONTENTS

LIST OF FIGURES

GLOSSARY

ABC	ATP binding cassette
ADP	Adenosine diphosphate
AEC	Adenylate energy charge
AMP	Adenosine monophosphate
ATP	Adenosine 5'-triphosphate
BSA	Bovine albumin serum
C	Celsius
$CaCl_2$	Calcium chloride
$CaCO_3$	Calcium carbonate
CO_2	Carbon dioxide
CYP450	Cytochrome P450
DMSO	Dimethyl sulfoxide
DOX	Doxorubicin
Fpgp	Fish P-gycoprotein
g	Gram
g	Acceleration of gravity
GSH	Glutathione
GST	Glutathione S-transferase
H_2SO_4	Sulfuric acid
HEPES	N- [2-hydroxyethyl] piperazine-N' [2-ethanesulfonic acid]

H	Hours
HSD	Highly significant difference
HSS	Hank's salt solution
I.U.	International units
KCl	Potasssium chloride
L	Liter
LDH	Lactate dehydrogenase
M	Molar
MDR	Multidrug resistance
MFO	Mixed function oxidase
$MgSO_4$	Magnesium sulphate
min	Minute
MRP	Multidrug resistance protein
MS222	3-Aminobenzoic acid ethyl ester methane sulphonate
MXR	Multixenobiotic resistance
NADH	β-Nicotinamide adenine di-nucleotide
$NaHCO_3$	Sodium bicarbonate
NaOH	Sodium hydroxide
NBDs	Nucleotide binding domains
O_2	Oxygen
PAH	Polycyclic aromatic hydrocarbon
PCB	Polychlorinated biphenyl

PEP	Phosphoenol pyruvate
P-gp	P-glycoprotein
Pi	Inorganic phosphate
PSM	Plant secondary metabolite
R123	Rhodamine 123
rpm	Revolutions per minute
SE	Standard error
Spgp	Sister P-glycoprotein
TAN	Total adenylate nucleotides
TMDs	Transmembrane domains
TX-100	Triton X-100
XR9576	Tariquidar

1.0 INTRODUCTION

1.1 Cellular defense strategies and their evolution

The continued exposure of organisms to natural and recently to anthropogenic chemicals, has lead to the evolution of cellular defense strategies to protect organisms against the harmful effects of such xenobiotics. These strategies can include biotransformation via phase I and II enzymes, and increased efflux of chemicals providing resistance to cells. In the later case, resistance is provided by active extrusion of conjugated metabolites of lipophilic compounds by a subset of ATP binding cassette (ABC) transport proteins, and active efflux of un-conjugated hydrophobic compounds mediated by the over-expression of ABC transport proteins termed multidrug (MDR) or multixenobiotic resistance (MXR) (Figure 1). All these defense strategies function to reduce intracellular accumulation of xenobiotics maintaining chemical homeostasis, which ultimately reduces the chance of toxic effects.

It is likely that cellular defence mechanisms evolved as a means of dealing with natural toxins such as plant secondary metabolites and animal toxins as well as endogenous compounds such as ions, sugars, amino acids, vitamins, peptides, polysaccharides, hormones, lipids (Malins and Ostrander, 1991). This suggests that these defense strategies first evolved to help animals cope with naturally occurring toxins and were later used to deal with new anthropogenic toxins, and highlights their importance in terms of fitness.

Plant and microbial secondary metabolites, and animal toxins are used for defence against predators, parasites and diseases, for interspecies competition and to aid in the reproductive process. Examples of such compounds include the plant secondary metabolites alkaloids, terpenes, and phenolics and animal toxins such as venoms and marine toxins (saxitoxin).

Throughout the 20th century we have seen the production of many new xenobiotic compounds such as dioxins, polychlorinated biphenyls (PCBs), polycyclic aromatic hydrocarbons (PAHs), pesticides, and for many of these compounds, the ultimate sink is the aquatic environment. This increasing development of anthropogenic toxins has lead to an increased exposure of aquatic animals to industrially-derived pollutants. Organisms were already equipped with cellular defence strategies to deal with natural toxins and used these same strategies to cope with an increasing environmental load of anthropogenic toxins

The early evolutionary development of cellular defense strategies is evidence of their importance in relation to increased fitness (Stegman, 1993). However, recent literature suggests that through maintenance and regulation, these systems may have significant energetic or metabolic costs to an organism.

All living systems, including fish, must conform to the first law of thermodynamics which states that matter and energy are never destroyed, only converted from one form to another (Brett and Groves, 1979). Fish gain energy through diet and lose energy through catabolism, which provides energy for maintenance and activity. In following the first law of thermodynamics, for body

weight to be maintained, energy gained through diet must equal energy lost through maintenance and activity. However, when energy requirements are not met, energy gained will not equal energy lost and therefore a reallocation of energy to process such as growth and reproduction is likely to occur, resulting in a net decrease in energy available to these processes which may ultimately affect an organisms overall fitness. This is especially true for juvenile fish that have very tight energy budgets due to the high cost of maintenance and activity (Wieser and Medgyesy, 1990). In a chemically stressful and energy limited environment, energy expenditures may be reallocated to provide for the additional cost of detoxification (Kitchell, 1983). These additional costs of detoxification are likely to be at the expense of other processes like growth and reproduction. Examining the costs of cellular defense mechanisms on systems such as growth and reproduction are important in understanding how these costs may affect the overall fitness of organisms. Two studies have suggested that there is a tradeoff between increased maintenance costs via detoxification and growth (Cresswell et al., 1992; Berenbaum and Zangeri, 1994) which studied the costs of detoxification of allelochemicals in insects. Furthermore, in 2004, Marchand et al. examined the relationship between "tolerant" and "sensitive" genotypes observed in contaminated European flounder (*Platichytys flesus*) populations and physiological parameters such as growth rate and fecundity as measures of fitness. They reported decreases in the relative fecundity and growth rate in contaminated populations, which was suggestive that survival in

such contaminated environments incurs energetic costs for fish, thus reducing energy available for other processes such as growth and reproduction.

1.1.1 Biotransformation

Xenobiotic biotransformation is the principal mechanism maintaining chemical homeostasis during organism exposure to xenobiotics (Klaassen and Watkins, 1999). Maintenance of chemical homeostasis or a constant chemical environment within cells in the face of dynamic chemical environments is important in preventing the accumulation of xenobiotics within cells, which can result in toxic effects

Biotransformation of xenobiotics maintains chemical homeostasis by reducing intracellular accumulation of compounds through detoxification and subsequent elimination. Enzymes capable of metabolizing xenobiotics are widely distributed throughout the body, being found in tissues such as skin, lungs, nasal mucosa, eyes, gastrointestinal tract, kidney, adrenal, pancreas, spleen, heart, placenta, testis, ovaries, and others (Klaassen and Watkins, 1999). In vertebrates, the liver contains the highest concentrations of xenobiotic metabolizing enzymes. The biotransformation processes convert lipophilic compounds into more water-soluble metabolites for excretion, and involve two types of reactions, categorized into phase I and II reactions.

Among the phase I reactions are oxidation, hydrolysis and reduction reactions, which expose or introduce a functional group. These reactions are catalyzed by a wide array of biotransformation enzymes, including the highly versatile cytochrome P450's (CYP450) and result in small increases in water

solubility (Klaassen and Watkins, 1999). Conversely, phase II reactions, which include glucuronidation, sulfation, acetylation, methylation, conjugation with glutathione (mercaptopuric acid synthesis) and conjugation with amino acids (such as glycine, taurine, and glutamic acid), and usually result in a large increase in the hydrophilicity of the xenobiotic, greatly promoting excretion (Klaassen and Watkins, 1999). During phase II reactions, functional groups that are present in xenobiotics or were introduced or exposed during phase I reactions, react with specific cofactors (Klaassen and Watkins, 1999). Xenobiotic biotransformation enzymes involved in phase II reactions are mainly found in the cytosol, whereas those involved in phase I reactions such as CYP450, are located primarily in the liver microsomes (Klaassen and Watkins, 1999).

Figure 1. Schematic diagram of cellular defense mechanisms in two adjacent hepatocytes: 1) biotranformation via Phase I reactions (e.g. hydroxylation via cytochrome P450, [CYP 450]) and Phase II reactions (e.g. conjugation via glutathione-s-transferase, [GST]), and 2) active efflux by multidrug resistance proteins (MRPs) and P-glycoprotein (P-gp) at the canalicular membranes (e.g. P-gp, and MRP2), and sinusoidal/basolateral membranes (e.g. MRP1, and MRP3). P-glycoprotein transport unmodified compounds out of the cell. MRP1 and MRP2 transport conjugated xenobiotics including organic anions and some unconjugated xenobiotics in the presence of glutathione (GSH). Substrates of MRP3 include anticancer drugs; some bile acid species; and several glucuronate, sulfate, and glutathione conjugates.

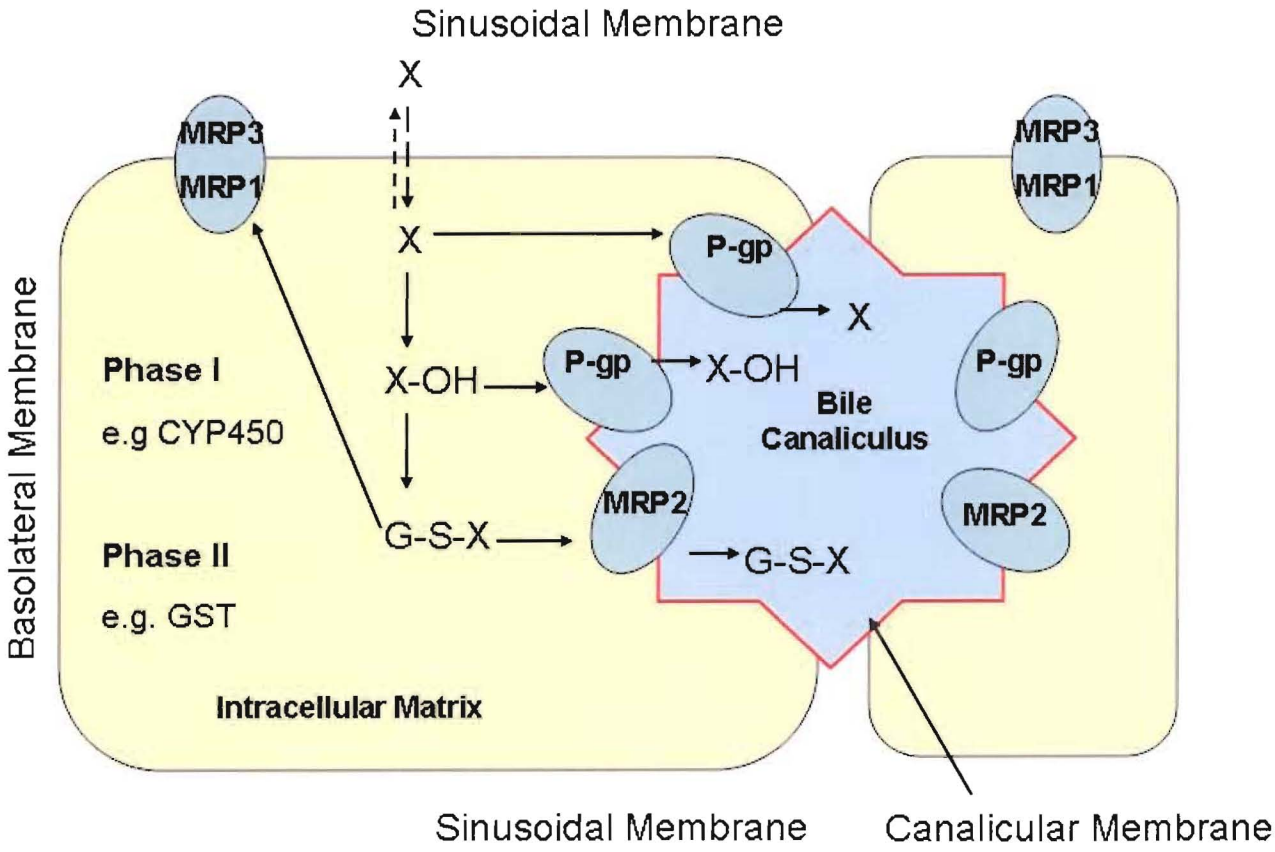
Sinusoidal Membrane
X
MRP3
MRP1
MRP3
MRP1
X
P-gp
X
Basolateral Membrane
Phase I
e.g CYP450
P-gp
X-OH
P-gp
X-OH
Bile
Canaliculus
MRP2
MRP2
G-S-X
Phase II
e.g. GST
G-S-X
Intracellular Matrix
Sinusoidal Membrane
Canalicular Membrane

1.1.2 Transport of conjugated lipophilic compounds

The active efflux of mercapturic acid (glutathione [GSH]) conjugates and other conjugated metabolites is mediated primarily by the multidrug resistance associated proteins (MRPs) MRP1, MRP2, and MRP3 belonging to the ABC superfamily of transport proteins (Jedlitschky et al., 1994). MRP1 and MRP2 transport organic anions, and mercapturic acid conjugates, and un-conjugated xenobiotics (vincristine, daunorubicin) in the presence of (GSH). MRP3 substrates include anticancer drugs, some bile acid species, and several glucuronate, sulfate, and mercapturic acid conjugates (Litman, 2001). MRP1 and MRP3 are located basolaterally transporting compounds into blood plasma whereas MRP2 is located at the canalicular membrane transporting compounds into the bile (Borst, 2000). MRP1 and MRP2 and have been shown to play a direct role in cellular defense by preventing accumulation of toxic conjugated and un-conjugated compounds (Litman, 2001).

1.1.3 Multidrug and multixenobiotic resistance

In addition to cellular defense via hepatic biotransformation and the efflux of conjugated lipophilic compounds, cells have also evolved a "first line of defence" (Epel, 1998), against xenobiotics which is referred to as multidrug (MDR) or multixenobiotic (MXR) resistance. Both MDR and MXR provide resistance through over-expression of ATP-binding cassette (ABC) proteins such as MRP1 and P-glycoprotein (P-gp), which reduce intracellular accumulation of xenobiotics.

Multidrug resistance was first described by Danø in 1973 who demonstrated that multidrug resistant (MDR) Ehrlich ascites cells were able to lower their intracellular daunorubicin concentrations by active drug efflux (Danø, 1973) through transmembrane active transporters belonging to the ABC superfamily. MXR in aquatic organisms is also mediated by the transport activity of transmembrane proteins belonging to the ABC superfamily (Higgins, 1992). Several experiments support the idea that over-expression of ABC transporters such as MRP1 and P-gp can prevent intracellular accumulation of xenobiotics, and therefore offer a protective role to the cells (Kurelec, 1989, 1991, 1992; Cornwall et al., 1995; Galgani et al., 1996; Kurelec, 1996; Minier et al., 1996).

The ABC superfamily includes more than 100 membrane transporters/channels that are involved in many functions including the uptake of nutrients, the transport of ions and peptides, cell signalling, and the extrusion of harmful compounds (Hennessy, 2007). Active extrusion of xenobiotics from cells by ABC transporters is powered by energy obtained from coupling ATP hydrolysis to drug transport (Endicott and Ling, 1988; Gottesman and Pastan, 1993). The best studied ABC transporters are the P-gps, encoded by the highly conserved multidrug resistance (MDR) gene family (Germann, 1996).

Two classes of mammalian MDR genes exist, which code for functionally different P-gps. Class 1 genes (human MDR1, mdr1a and mdr1b in rats), confer inducible xenobiotic resistance, whereas Class 2 genes encode an un-inducible phosphatidylcholine translocator (Bard, 2000). Many organisms have been shown to posses these multidrug transport proteins including bacteria, plants,

yeast, invertebrates, and vertebrates (Croop, 1993). The search for similar multidrug resistance proteins in aquatic organisms began by Kurelec *et* al. in 1989 in hopes to uncover similar mechanisms of cellular defense in aquatic species. Highly conserved MDR genes have been described in several aquatic organisms including winter flounder *Pleuronectes amaricanus* (Chan et al., 1992), Killifish, *Fundulus heteroclitus* (Cooper et al., 1996). In addition, P-gp proteins have been described in various organs in several fish species (Hemmer, 1995; Kleinow, 2000). Two fish P-gp (fpgpA and B) genes have been partially cloned in winter flounder and killifish (Chan et al., 1992). FpgpA corresponds to the liver specific sister gene of p-gp (spgp) which does not play a role in drug resistance, while fpgpB is related to both Class 1 and 2 mammalian P-gps (Cooper et al., 1996).

1.1.3.1 P-gp substrates and modulators

P-gp substrates differ in cytologic target, chemical structures, and properties (Endicott and Ling, 1989). However, some physical similarities do exist between P-gp substrates such as being moderately hydrophobic, amphipathic, low molecular weight, planar molecules (Gottesman and Pastan, 1988; Endicott and Ling, 1989). P-gp substrates include chemotherapeutic drugs such as cholchicine, vinka alkaloids (e.g. vinblastine, vincristine), actinomycin D, taxol, epipodophyllotoxins, calcium channel blockers (e.g. verapamil), antiarrhythmics (e.g. quindine), antihypertensives (e.g. reserpine), steroids (e.g. cortisol, aldosterone), antiparasitics (e.g. quinine, ivermectin) and anthracyclines (e.g. doxorubicin) (Bard, 2000).

Doxorubicin (DOX) is and anthracylcine anticancer drug used widely in the treatment of cancer (Wadler et al., 1986) and is an established P-gp substrate (Wacher, 1995; Sturm, 2001). DOX is known to be cardiotoxic (Lefrak et al., 1973) although the mechanism is unclear. DOX is primarily metabolized by the liver and is excreted into the bile (Ballet et al., 1987). DOX is known to enter cells by passive diffusion through the lipid bilayer (Gallois, 1998). DOX like other anthracyclines is amphiphilic with the amino sugar moiety bearing the positive electrostatic force which interacts with the polar head groups of the lipid bilayer (Gallois, 1998). There is evidence that the primary circulating metabolite of DOX, Doxorubicinol plays a key role in DOX associated cardiotoxicity. Studies suggest that DOX induced cardiotoxicity may result from the formation of free radicals that stimulate lipid peroxidation and alter cellular integrity (Singal et al, 2000; Olson et al, 1990). Other studies have suggested that the mechanism behind DOX induced toxicity may be related to inhibition of DNA synthesis (Geiwirtz, 1999), DNA intercalation (Tanaka & Yoshida, 1980), or induction of enzymatic or chemically activated DNA adducts (Cullinane et al., 1994).

A group of structurally unrelated compounds known as reversing agents or modulators (Ambudkar et al, 1999) causes inhibition of P-gp-mediated drug transport. Some P-gp modulators are themselves substrates and therefore inhibit drug efflux through competitive inhibition with a substrate, whereas the inhibitory mechanism for many other P-gp modulators is still unknown. Recently it has been suggested that the mechanism of action for several P-gp modulators is through an allosteric mode of action. In 1999, Martin et al., examined the

inhibitory action of tariquidar (XR9576), an anthranilic acid derivative, and found that it was not through physical competition with the substrate but rather through an allosteric effect on ATP hydrolysis or substrate recognition. XR9576 binds with high affinity to the P-gp transporter, and potently inhibits activity (Roe et al., 1999; Martin et al., 1999; Mistry, 2001; Walker et al., 2004).

Recent work in trout hepatocytes has demonstrated the inhibitory ability of XR9576 on P-gp mediated efflux, and as such, XR9576 was used in the present study to inhibit doxorubicin mediated P-gp transport. Bains and Kennedy, 2005 found an increase in respiratory rates associated with P-gp mediated rhodamine 123 (R123) efflux and demonstrated that XR9576 significantly inhibited R123 efflux with a concomitant return of respiration rates to baseline values.

1.2 Energetic costs of cellular defense

Exposure of cells to the selection pressure of cytotoxic drugs has led to the development of cellular defense mechanisms such as hepatic biotransformation, active export of conjugated xenobiotics and metabolites, and multidrug (MDR) and multixenobiotic resistance (MXR). Under these conditions, several changes in the cell may be observed. These changes may include induction and over expression of drug transporters, such as P-gp, and MRP (Albertus and Laine, 2001; Gottesman and Pastan, 1993; Bard, 2002), and enzymes involved in phase I and II detoxification systems such as CYP450 (Bard, 2002), or take the form of MDR supporting mechanisms such as

acceleration of ATP generating processes such as cellular respiration (Bains and Kennedy, 2004; 2005).

Through the maintenance and regulation of cellular defense mechanisms it is likely that energetic and nutritive costs will be imposed on organisms. All organisms tend to have a relatively fixed energy budget (Maryanski et al., 2002) which depends on the relationships between the acquisition and allocation of energy to an array of biological, biochemical, and physiological processes within an organism (Xie and Sun, 1993). In considering that the energy budgets of organisms is fixed, an increase in the requirement for energy for one biological process will cause a reduction in the energy available to other processes, with the most energy available to those with an effect on immediate survival (Brett and Groves, 1979).

Such costs may include those associated with biotransformation and excretion (Bains and Kenndy 2004, 2005), maintenance of acid-base balance altered by the production of acidic metabolites (Foley, 1992, 1995), active efflux of xenobiotics by ATP-dependent drug efflux pumps such as P-gp (Bains and Kenndey, 2005), as well as long-term costs associated with physical alterations of the tissues or organs involved in detoxification (Hinton and Lauren 1990; Rubin and Lieber 1974).

Costs associated with cellular defense represent energetic costs, which may limit energy available to other biological and physiological processes in an organism. The effect of energy usage by cellular defense mechanisms on the energy budgets of organisms is poorly understood, however, studies have

suggested that the cost of cellular defense may be significant and disadvantageous to other processes like growth and reproduction since there is the likelihood of a decrease in the energy allocation to these processes (Foley, 1992).

1.3 Potential mechanisms

1.3.1 Biotransformation

The ability to metabolize xenobiotics is essential for the survival or organisms, however, through phase I functionalization and phase II conjugation reactions, significant energetic and nutritive costs may be imposed on organisms. Phase I reactions, require reducing equivalents of NADPH and result in an increase in energy and molecular oxygen used in enzymatic conversions (Klaassen and Watkins, 1999). Phase II reactions require the use of enzymes such as glucuronosyl and sulfotransferases, which use energy for the activation of substrates, while others such as glutathione (GSH) S-transferase (GST) require energy for the synthesis of GSH (Klassen and Watkins, 1999). Several recent studies have examined the energetic costs of hepatic biotransformation and P-gp transport of xenobiotics in trout hepatocytes and have suggested that both incur higher energetic costs to organisms exposed to environmental toxins when compared to unexposed groups (Bains and Kennedy, 2004; Bains and Kennedy 2005). In 2004, Bains and Kennedy examined energetic costs associated with pyrene metabolism in isolated trout hepatocytes. Since pyrene is non toxic, they were able to attribute increased respiratory rates in hepatocytes incubated with pyrene to xenobiotic metabolism.

1.3.2 Maintenance of acid-base balance

Extracellular and intracellular acid-base balance is necessary for the maintenance of normal metabolic processes. The production of large acid loads through biotransformation and metabolism of compounds can threaten acid-base homeostasis, and there is evidence that there are costs in dealing with large acid loads produced from the biotransformation and metabolism of xenobiotics such as plant secondary metabolites (PSM) (Foley, 1992, 1995).

Disturbances of acid-base balance show wide-ranging effects on biochemical and physiological processes of animals including effects on organ systems (respiratory, cardiovascular, and skeletal), whole body homeostasis, and metabolism of carbohydrates, proteins and nitrogen (Foley, 1995). Organic acids are dealt with by being buffered and removed from the body which is suggested to be energetically costly to an organism (Foley, 1992).

In herbivorous animals, such as birds and mammals, consumption of PSM results in an acid load and has been shown to have significant metabolic effects (Foley, 1992). The effects of acid loads on animals are well understood and there are clear links between dietary acid loads and energy balance. Work by Cresswell et al. in 1992 demonstrated that detoxification of dietary nicotine exacts a fitness loss and imposes a metabolic cost on the southern army worm (*Spodoptera eridania*). Studies with insects have confirmed that insecticide resistance constitutes energetic costs to organisms. Decreased overwintering success of insecticide resistant individuals was identified in *Lucilia cuprina* and *Myzus persicae* (Mckenzie, 1994; Foster et al., 1999) indicating a possible fitness

cost linked to the energetic balance of insects. Other work in insects has shown differences in mating success and predation risk in *Culex pipens* L. and mating success, fecundity, and development time in *Cydia pomonella* L. (Bovin et al., 2001; Berticat et al., 2002, 2004). Work in vertebrate herbivores has suggested that PSMs exact significant nutritional costs to herbivores either by affecting nutrient utilization (Glick and Joselyn, 1970 a, b; Robbins et al., 1987a, b) or by imposing high detoxification costs post absorption (Dash, 1988). Furthermore, work in vertebrate foraging behaviour in the ruffed grouse indicated substantial metabolic costs of detoxifying ingested PSMs, which were reduced by selective foraging (Guglielmo, 1996).

1.3.3 Efflux pumps

In addition to the protective role of drug transporters such as MRP and P-gp, it is suggested that through the active transport of xenobiotics, this activity may be costly to organisms. Several studies have begun to examine the costs associated with P-gp transport activity and have provided evidence that these costs may be substantial.

P-gp mediated transport of substrates is driven by the energy coupled from ATP hydrolysis. Several reports have shown that the ATPase activity of P-gp is important for drug transport, although the mechanism by which ATP hydrolysis is coupled to drug transport is still unclear. It is believed that coupling between P-gp transport and ATP hydrolysis involves a transient conformational change in the protein that facilitates an interaction between the drug binding domain and nucleotide binding sites of P-gp (Litman et al., 2001). Unlike other ABC proteins,

P-gp exhibits a high level of basal ATPase activity in the absence of drugs. The basal activity may be caused by transporting endogenous lipids or hydrophobic peptides (Sharom et al., 1995). ATPase activity that is uncoupled from substrate transport may also contribute to the basal activity (Ambudkar et al., 1999).

Recent work in trout hepatocytes (*Oncorhynchus mykiss*) examining the effects of P-gp mediated transport of R123 on cellular respiration revealed that increased P-gp transport of R123 significantly raised cellular respiration rates (Bains and Kennedy, 2004, 2005). Basal respiration rates in hepatocytes exposed to 5 and 10 μM R123 increased by 18.5 and 25.7%, respectively, which translates into substantial costs associated with P-gp transport.

1.4 Using adenylate nucleotides as measures of energy use

Adenylate nucleotides play a central role in metabolism, acting as a link between energy-yielding and energy-utilizing processes in the cell. It is well known that without adequate supplies of energy, cells rapidly die (Calderwood et al., 1985). Energy-linked cytoxicity may occur through deprivation of energy production substrates, or through the inhibition of energy yielding processes such as glycolysis or respiration in the cell (Calderwood et al., 1985). Cells utilize adenylates as common chemical intermediates for efficient coupling of energy-producing and energy-consuming processes (Lehninger, 2005, 1965). Concentrations of ATP, AMP, and ADP have been widely used to monitor energy status, metabolic activity, physiological stress, etc. in a broad range of cell types and tissues (Nilsson et al., 1975; Calderwood et al., 1985; Zaroogian 1989;

Fedorow et al., 1998; Kohane and Watt, 1999). Adenylates interact either directly or indirectly with all aspects of cell metabolism, taking part in phosphotransferase reactions and controlling enzyme reactions (Lehninger, 1965; Atkinson, 1997).

Measuring ATP concentration alone appears to be inadequate as an overall indicator of cell energy balance (Atkinson, 1977; Slater, 1979). However, adenlyate ratios such as adenylate energy charge (AEC), and phosphorylation potential (PP) have been shown to be better indicators of cellular energy status (LeBras, 1995; Li et al., 2005; Overgaard and Gesser, 2004). AEC is an indicator of the degree of phosphorylation of the ATP-ADP-AMP system, and is calculated from the following ratio: AEC = [ATP] + 0.5[ADP]/[ATP] + [ADP] + [AMP]. AEC has a maximum value of 1.0, when all adenylate is in the form of ATP, and a minimum value of 0 when all adenylate is in the form of AMP. Cells appear to maintain AEC at a value of approximately 0.85 (Atkinson, 1977; Pradet and Raymond, 1983.) AEC values correlate with physiological condition: values between 0.8 and 0.9 are typical of organisms, which are actively growing and reproducing under optimal environmental conditions (Chapman et al., 1971; Atkinson, 1971). Values from 0.6 to 0.7 have been observed in organisms, which are stressed (Ball & Atkinson, 1975; Behm and Bryant, 1975, LeBras, 1995). AEC values below 0.5 indicate cell death (Ridge, 1972; Montague & Dawes, 1974). The cell stabilizes its energy charge by adjusting the rate of ATP synthesis to the state of energy demand. A decrease in the energy charge leads to activation of ATP generating processes. When energy requirements can not

be met, the AEC drops, which leads to an increase in the AMP concentration. AMP deaminase degrades AMP, thereby increasing AEC.

Toxicant exposure is known to affect adenylate energy charge in several aquatic and mammalian species. For example LeBras, 1995, provided evidence that a decrease in AEC in whole body extracts of the aquatic invertebrate *Asellus aquaticus L.* from lindane exposure (4 and 8 mg/l) for 48 h was indicative of an increased energetic cost and metabolism, resulting from the hyper-excitability characteristically induced by this type of contaminant. Exposure of the mussel *Mytilus edulis* to dredged material for 28 days containing PCBs (39 ng/g, PAHs (4500 ng/g) and metals Cu and CR at 60 and 50 µg/g dry weight was shown to significantly lower AEC in extracts from adductor muscles compared to controls (Zaroogian, 1989). AEC, was also found to be lower compared to controls in whole body extracts of the shrimp *Palaemonetes varians* when exposed to 0.5 mg/L of ammonia over a period of 14 days (Marazza and Le Gal, 1996). Finally, significant decreases in AEC were observed in muscle extracts from the bivalve *Cerastoderma edule* submitted to sub-lethal concentrations of paper mill effluent (Picado, 1990). Furthermore, work with rat hepatocytes, examined the protective effects of isoflurane on energy balance by measuring adenylate nucleotides and adenylate energy charge (Li et al., 2005) and found that isoflurane partly prevented decreases in both energy charge and total adenine nucleotide during anoxia and reoxygenation. All these results indicated that toxicant exposure can have effects on AEC which has been shown to be indicative of energy use.

Therefore, measuring toxicant induced reductions in AEC can be used as a measure of energy use.

PP is calculated from the ratio: [ATP]/[ADP] [Pi] and is considered a more sensitive indicator of the energy status of a cell than energy charge (Lehininger, 2005, 1975). Studies have demonstrated that this ratio is maintained at approximately 100-200 M^{-1} in mammalian cells (Wilson et al., 1974 a,b; Hassinen and Hiltunen, 1975), and between 200 and 800 M^{-1} in other cell types (Lehininger, 2005, 1975). The phosphorylation potential is a measure of the potential of the cell for carrying out ATP-dependent processes (Lehininger, 2005) and varies depending on the metabolic state of the cell, with higher values indicative of a more highly "energized" cell (Lehininger, 2005, 1975).

1.5 Objectives of the study

The overall objective of this study was to functionally and energetically characterize P-glycoprotein transport activity in rainbow trout hepatocytes. Specifically, this study examined the P-gp-mediated efflux of DOX, a fluorescent substrate of mammalian mdr1-type P-gp, in the presence and absence of the third generation inhibitor XR9576. Furthermore, this study quantified the energetic costs associated with P-gp transport of DOX via the use of adenylate nucleotide measurements.

2.0 MATERIALS AND METHODS

2.1 Fish

Rainbow trout (*Oncorhynchus mykiss*) were obtained from Miracle Springs Trout Farm (Mission, BC). Trout of both sexes weighing between 600-800g were housed in 1200L tanks at Simon Fraser University (Burnaby, BC) supplied with a flow-through system of well oxygenated, dechlorinated water at 15°C. Hardness of the water was 4 mg $CaCO_3$/L and pH was 6.7. Fish were acclimated for up to 2 weeks prior to experimentation and fed with Pro-Farm floating Koi food from EWOS Canada (Surrey, BC).

2.2 Chemicals

Type IV collagenase, N- [2-hydroxyethyl] piperazine-N' [2-ethanesulfonic acid] (HEPES), Hank's balanced salts (product #H4891), bovine albumin serum (BSA), $MgSO_4$, for the preparation of HSSA, HSSB, and HSSC were purchased from Sigma Chemical Co. (St. Louis, MO). 3-Aminobenzoic acid ethyl ester methane sulphonate (MS222), doxorubicin (DOX), tritonX-100, (TX-100), reduced β-Nicotinamide adenine di-nucleotide (NADH), trypan blue, and pyruvic acid were ordered from Sigma Chemical Co. (St. Louis, MO). $CaCl_2$ and $NaHCO_3$ were purchased from Fisher Scientific (Fair Lawn, NJ), and Merck KgaA (Darmstadt, Germany), respectively. XR9576 was donated by Rob Robey and David Norris.

For the conversion of ADP to ATP by the pyruvate kinase reaction, and AMP to ATP via the myokinase reaction phosphoenolpyruvate, KCl, $MgSO_4$, myokinase (from rabbit skeletal muscle), and pyruvate kinase (from rabbit skeletal muscle), and tricine buffer were purchased from Sigma Chemical Co. (St. Louis, MO). Pyruvate kinase was obtained in lyophilized form, and myokinase as a suspension in ammonium sulphate.

The ATPLite™ luminescence ATP detection system used to determine intracellular ATP concentrations was obtained from PerkinElmer Life Sciences (Woodbridge, Ontario, Canada).

For the quantitative colorimetric phosphate determination in samples, the Quantichrome™ Phosphate Assay kit (DIPI-500) was ordered from BioAssay Systems (Hayward, CA).

2.3 Hepatocyte isolation

Each hepatocyte isolation required the preparation and use of three solutions containing Hank's balanced salts (HSSA, HSSB and HSSC) (Moon et al. 1985). Preparation of all solutions began by combining Hanks' Balanced Salts (HBSS from SIGMA), 2.603g HEPES, and 0.0976 g $MgSO_4$ with 1L ultra filtered water. This solution (HSSA) was then gassed with a mixture of 1% CO_2 and 99% O_2 (Praxair Products Inc., Mississauga, ON) for 60 min on ice. Following this, 0.35g $NaHCO_3$ was added and the pH was adjusted to approximately 7.6 at 20°C by the addition of either 1 N H_2SO_4 or 1 N NaOH. Following the pH adjustment, HSSB was prepared by dissolving 20g/L BSA and

0.185 g/L $CaCl_2$ in HSSA. Similarly, HSSC was then prepared by dissolving 0.6g/L of Type IV collagenase in HSSA. During experimentation all solutions were kept on ice.

Trout were anesthetized in dechlorinated water containing 0.2 g/L MS222 buffered with 0.2 g/L $NaHCO_3$. Cessation of opercular movement was used as an indication of the proper level of anaesthesia. Following anaesthesia, mass was recorded and trout were transferred to an area prepped for the isolation of hepatocytes.

Isolation of hepatocytes was performed according to Bains and Kennedy (2004) which was slightly modified from Moon et al., (1985). A ventral incision was made from the pectoral fins to the gills followed by an incision on each side behind each pectoral fin to exposing the liver. The heart was located and cut after which cold HSSA was pippetted over the area. Blood vessels leading from the liver to the heart were then cut, and the hepatic portal vein was cannulated with a syringe head connected to a peristaltic pump (Cole-Parmer Instrument Co). The liver was first perfused with HSSA at a flow rate of 2 ml/min/g of liver until the blood was cleared, from the liver (approximately 15 min). Following this, the liver was perfused with HSSC until the first signs of disaggregation. During perfusion with both HSSA and HSSC, the liver was gently massaged and kept cool by pipetting ice-cold HSSA over it. The cannulating syringe was then removed, and the liver was cut away from the fish and gall bladder. The liver was then placed in a on watch glass on ice, containing HSSA and gently minced with a razor blade. Next, the liver pieces were pressed through a screen of nylon

mesh (253 µm) followed by washing through a second screen (73 µm) with HSSA. The cell suspension was then poured into 15 ml polypropylene conical tubes and kept on ice until used.

Hepatocytes were then collected by centrifugation at 42 x *g* for 4 min at 4°C using a centra MP4R centrifuge (International Equipment Co., Needham Heights, MA). The supernatant was removed and cells were re-suspended in ice-cold HSSB and washed to remove any cell debris. Again, the supernatant was removed and the cells pellets were re-suspended in HSSB and placed on ice. A 1ml aliquot of the hepatocyte suspension was transferred into a pre-weighed 1.5 mL eppendorf tube and was centrifuged at 3700 x *g* for 3 min. The concentration of hepatocytes in mg/ml was determined in the final solution by removing the supernatant and weighing the cells (Siebert, 1985). Cells were seeded at a density of 10 mg/ml.

2.4 Cell viability and cytotoxicity

During each hepatocyte isolation, cell viability was assessed by trypan blue exclusion at various time points throughout the experiment according to the method of Gill and Walsh (1990). Briefly, 50 µl of cell suspension was combined with 50 µl of trypan blue (0.4% solution) in a 1.5 mL eppendorf tube, and 9 µl of this was then transferred to a hemocytometer. Cells stained blue were counted as dead cells, and clear cells were counted as alive. The percent viability was calculated from these numbers.

In order to assess potential damage caused to cell membranes due isolation, or exposure to either doxorubicin (DOX) or tariquidar (XR9576), a lactate dehydrogenase (LDH) leakage assay was conducted in 6 separate fish, following modified protocols from Nicholson (1994), and Pesonen and Anderson (1992). LDH activity was measured in cell suspensions (10mg/ml viable cells) in HSSB containing DOX (0, 5, 25, 125, 250 µM) or XR9576 (300nM), or 1% TX-100 as a positive incubated for 0 and 4 hrs. The blank consisted of HSSB without cells. The first LDH reading was taken at 0 hr with the treatment on ice and then at 4hrs after incubating at 12°C which was the acclimation temperature of the trout during the time of the experiment.

The wavelength of the Milton Roy Spectronic 301 spectrophotometer (Mahin & Associates, Reno, NV) was set to 340 nm and auto-zeroed with 3 ml of reference solution (HSSB). Three ml of HSSB and 50 µl of one of the treatments, except for the Triton X-100 treatment (where only 35 µl was added), was placed into the spectrophotometer for recording of absorbance at 340 nm. Damaged cells release LDH, which leads to a decrease in NADH. Therefore, cell damage is estimated by the decrease in absorbance related to declining levels of NADH. The rate of decline in absorbance/min was used to measure LDH activity, where a greater rate of decline translates into a higher LDH acitivty.

2.5 Accumulation and efflux of doxorubicin

Accumulation experiments were performed according to Bains and Kennedy (2004) which was modified from Sturm et al., (2001). Aliquots of cell

suspension were combined with HSSB to achieve final a final cell concentration of approximately 10 mg cells/ml and were gently mixed on a Maxi Mini III vortex mixer. Cells were pre-incubated for 60 min at 12°C before the addition of 5µl DOX in DMSO to achieve final DOX concentrations of 5, 25, 75 and 125 µM. At 0, 5, 10, 15, 30, 60 and 120 min, cell suspensions were centrifuged at 42 x *g* for 3 min and the supernatant removed. Intracellular accumulated DOX was extracted three times from pelleted cells with 2 ml of *n*-butanol. After each addition of *n*-butanol, cells were shaken on a reciprocating shaker for 1 hr at room temperature. DOX concentrations were measured using a Cary Eclipse Flourometer at excitation and emission wavelengths of 470 and 585 nm respectively. DOX concentrations were quantified using a range of prepared doxorubicin standards of 6.25, 3.13, 1.56, 0.78, and 0.39 µM, which were linear over the entire range.

In efflux experiments, cells were allowed to accumulate DOX as described above for 60 min, after which cell suspensions were centrifuged at 42 x *g* for 3 min. The supernatant was removed and cells washed twice with HSSB, re-suspended in fresh HSSB, and incubated for various time periods (0, 5, 10, 15, 30, 60, 120 min). After incubation, cell suspensions were removed and centrifuged at 42 x *g* for 3 min and the supernatant was removed. DOX was extracted from cells and supernatant, and DOX concentration was determined as described above.

For the efflux experiments with XR9576-treated hepatocytes, a similar protocol was used as in the efflux experiments. XR9576 was added to cell

suspensions following 45 min acclimation period to achieve a final concentration of 300 nM, which has previously been shown to significantly inhibit P-gp in the drug resistant tumor cell line NCI/ADR^{Res} (Walker et al., 2004). These cells were incubated for a further 15 min. Hepatocytes were then incubated with DOX for 60 min to 'pre-load' cells with DOX. Following this, cells were washed twice in HSSB, and re-suspended in DOX-free media for time periods of 0, 5, 10, 30, 60, and 120 min. Cell suspensions were centrifuged at 42 x *g* for 3 min to remove supernatant. Intracellular DOX was extracted and analyzed for DOX as described above.

2.6 Adenylate nucleotides

ATP concentrations were determined using the ATPLite^{TM} bioluminescence detection system (PerkinElmer Life Sciences) which is an adenosine triphosphate (ATP) monitoring system based on firefly (*Photinus pyralis*) luciferase. The PerkinElmer ATPlite ^{TM} assay system was chosen due to its major advantages which include high sensitivity, excellent linearity, simplicity, relatively fast results and the lack of cell harvesting or separation steps. Another advantage of this system is that the lysis solution, which releases the ATP, irreversibly inactivates the endogenous ATP degrading enzymes (ATPases) by raising the pH. The subsequent addition of the substrate solution (Luciferase/Luciferin) lowers the pH to a suitable level so that the reaction can occur. The ATPLite ^{TM} assay system is based on the production of light caused by the reaction of ATP with added luciferase and D-luciferin, with the amount of

light emitted being proportional to the ATP concentration. The ATPlite™ monitoring system has been used to assess the cytocidal, cytostatic and proliferative effects of a wide range of drugs, biological response modifiers and biological compounds (Kangas et al., 1984; Lundin et al., 1986; Crouch et al., 1993; Petty et al., 1995; Storer et al., 1996; Cree and Andreotti, 1997).

The ATPLite ™ assay was performed in 96-well culture treated assay plates (PerkinElmer Life Sciences) with 100 µl cell suspension/well (10mg cells/ml). Lyophilized substrate buffer solution was dissolved in substrate buffer solution and agitated gently to achieve a homogenous solution. The reagents were then allowed to equilibrate to room temperature before beginning the assay. Lysis solution (50 µl) was added to 100 µl of cell suspension per well. The microplate was then shaken gently on an orbital shaker for 5 min at 700 rpm. Next, 50 µl of reconstituted substrate (luciferin/luciferase solution reconstituted witih substrate buffer solution) solution was added to each well, and the plate was again shaken on an orbital shaker for 5 min at 700 rpm. The plate was then dark-adapted for ten minutes and luminescence was then measured on a PerkinElmer Victor Microplate Reader (PerkinElmer Life Sciences, Ontario, Canada).

An ATP standard curve was prepared in the same microplates that were used for experimental samples following manufacture's protocols as described above. ATP standard was dissolved in water to obtain a 10 mM stock solution. The vial was swirled gently for one minute to allow the ATP to dissolve

completely. A dilution series in water was prepared from a concentration of 1 x 10^{-5} M down to blank.

For the determination of ADP concentration in samples, ADP was converted to ATP following a method by Gorman et al., (2003). ADP was converted to ATP using the pyruvate kinase reaction. Samples were thawed and cells were lysed using the lysis solution provided with the ATPlite ™ detection system (Perkin Elmer Life Sciences) by combining 100 µl cell suspension with 50 µl lysis solution. In a 1.5 mL eppendorf tube, 100 µl of cell suspension was added to 300 µl of a solution containing 40 U/mL pyruvate kinase, 40 µmol/L PEP, and 10 mmol/L KCl in 40 mmol/L tricine buffer, pH 7.75. Conversion of ADP to ATP was complete after 5 min at room temperature. After the 5 min incubation, ATP (representing ATP + ADP) was measured using the ATPlite™ bioluminescent kit (Perkin Elmer Life Sciences) following manufacturer's protocol as described above.

AMP was converted to ADP which was then converted to ATP by adding myokinase (100 U/mL) to the above solution. Samples were thawed and cells were lysed using the lysis solution provided with the ATPlite ™ detection system (Perkin Elmer Life Sciences) by combining 100 µl cell suspension with 50 µl lysis solution. In a 1.5 mL eppendorf tube, 100 µl of cell suspension was added to 300 µl of a solution containing 40 U/mL pyruvate kinase, 100U/mL myokinase, 40 µmol/L PEP, and 10 mmol/L KCl in 40 mmol/L tricine buffer, pH 7.75. Conversion of AMP to ATP was complete after 120 min at room temperature. AMP (representing ATP + ADP +AMP) was measured using the ATPlite™

bioluminescent kit (Perkin Elmer Life Sciences) following manufacturer's protocol as described above.

2.7 Inorganic phosphate

Intracellular concentrations of inorganic phosphate (Pi) in samples was determined using the Quantichrom™ Phosphate Assay Kit (BioAssay Systems; Hayward, CA) (Ekman and Jager, 1993; Fisher and Higgins, 1994; Cogan, 1999).

The BioAssay System's kit is designed to measure phosphate ions directly in samples without any pretreatment. The assay utilizes the malachite green dye and molybdate, which forms a stable colored complex specifically with inorganic phosphate. Color intensity is measured at 620 nm and is directly proportional to the phosphate concentration in the sample.

A serial dilution from 30 µM down to blank, in water was used to make a set of standards (30, 25, 20, 15, 10, 5 and 0 µM). Reagents were allowed to equilibrate before beginning the assay. Once reagents reached room temperature, 50 µl of distilled water (blank), standard and samples were transferred in duplicate wells of a clear bottom 96-well plate. Next, 100 µl of malachite green reagent was added to each well and the microplate was tapped lightly to mix. The plate was incubated at room temperature for 30 min after which the optical density was read at 620 nm.

2.8 Statistical analysis

Statistical analyses were performed using the JMP IN 5.0.1 program (SAS Institute Inc., Cary, NC). Results were expressed as means $\pm$ SE.

DOX accumulation and efflux rates between treatments were compared using a single factor analysis of variance and Tukey-Kramer highly significant difference (HSD) test in a single-factor randomized complete block design (α = 0.05).

LDH activity and cell viability between treatments was compared using a two-factor analysis of variance and Tukey-Kramer HSD test in a two factor (6x2) split plot in time analysis of variance (α = 0.05). The two factors were time period with two levels (0, 4hrs) and exposure treatment groups with 6 levels (HSS B control, 1% TX-100, as well as 0, 25, 125 µM DOX, and 300 nM XR9576).

Comparison of ATP, ADP, AMP, Pi, adenylate energy charge (AEC), and phosphorylation potential (PP) between treatments during the accumulation and efflux period of the experiment were also done using a two-factor analysis of variance and Tukey-Kramer HSD test in a two-way (9x3) split plot in time analysis of variance (α = 0.05).

For comparison during the accumulation phase, the two factors were exposure treatment groups, with 3 levels (0 µM DOX, 125 µM DOX, 125 µM DOX + 300 nM XR9576) and time with 4 levels (0, 20, 40, 60 min.) For comparison during the efflux phase, the two factors were exposure treatment groups, with 3 levels (0 µM DOX, 125 µM DOX, 125 µM DOX + 300 nM XR9576) and time with

5 levels (70, 80, 100, 130, 190 min post accumulation.) Differences were considered significant at $p \leq 0.05$.

3.0 RESULTS

3.1 Cell viability and cytotoxicity

Results from the trypan blue exclusion and lactate dehydrogenase (LDH) leakage assay and are shown in Fig. 2 and 3. No significant differences were seen in cell viability using trypan blue exclusion between control and doxorubicin (DOX) or tariquidar (XR9576)-exposed hepatocytes for incubations up to 240 min (range: 81.8 $\pm$ 1.6 to 88.8 $\pm$ 0.8 % viable cells). A significant difference in cell viability was observed with the Triton X-100 (TX-100) positive control compared to all other treatments ($p<0.001$). No significant differences between control and DOX or XR9576-exposed cells were seen in LDH activity (range: 154.6 ± 9.6 to 258.3 $\pm$ 19.2 IU/L). Significantly higher LDH activity was seen with the TX-100 positive control compared to all other treatments ($p<0.001$).

3.2 Doxorubicin accumulation and efflux

P-gp-mediated DOX accumulation and efflux were characterized in rainbow trout hepatocytes in order to correlate changes in cellular adenylates, inorganic phosphate, adenylate energy charge, and phosphorylation potential with P-gp transport activity. To characterize this activity, the dynamics of DOX kinetics in isolated hepatocytes exposed to varying concentrations of DOX and the P-gp inhibitior XR9576 were examined. At all DOX incubation

Figure 2. Cell viability of hepatocytes from treatment groups at 1 (■) and 4 hour (▒) post incubation periods. Treatment groups were: dimethylsulfoxide (DMSO) as a negative control, TX-100 as a positive control, 300 nM XR9576, and DOX at concentrations of 5, 25, 75 and 125 μM. No significant differences were seen in cell viability between control, DOX or XR9576-exposed hepatocytes for up to 240 min. Cell viability was significantly lower (*) for the TX-100 treatment at both incubation times compared to all other treatment groups ($p<0.001$). Values are means + SEM., *n=6*.

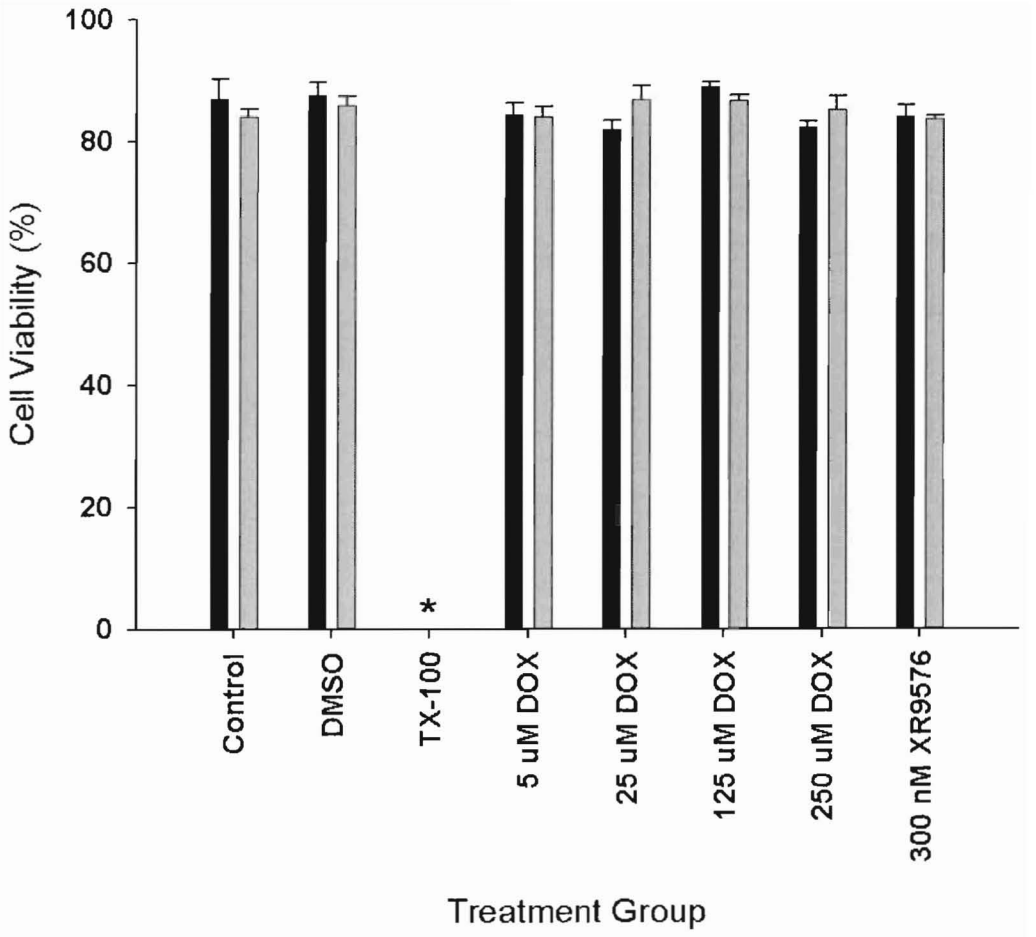
100
80
60
40
20
0
Cell Viability (%)
*
Control
DMSO
TX-100
5 uM DOX
25 uM DOX
125 uM DOX
250 uM DOX
300 nM XR9576
Treatment Group

Figure 3. Extracellular LDH enzyme activities of hepatocytes from treatment groups after 1 (□) and 4 hour (■) post-incubation periods. Treatment groups were: dimethylsulfoxide (DMSO) as a negative, dimethylsulfoxide (DMSO), TX-100 as a positive control, XR9576, and DOX at concentrations of 5, 25, 75 and 125 μM.). No significant differences between control, and DOX or XR9576-exposed cells were seen in LDH activity. LDH activity was significantly higher (*) for the TX-100 treatment at both incubation times compared to all other treatment groups ($p<0.001$). Values are means + SEM., *n=6*.

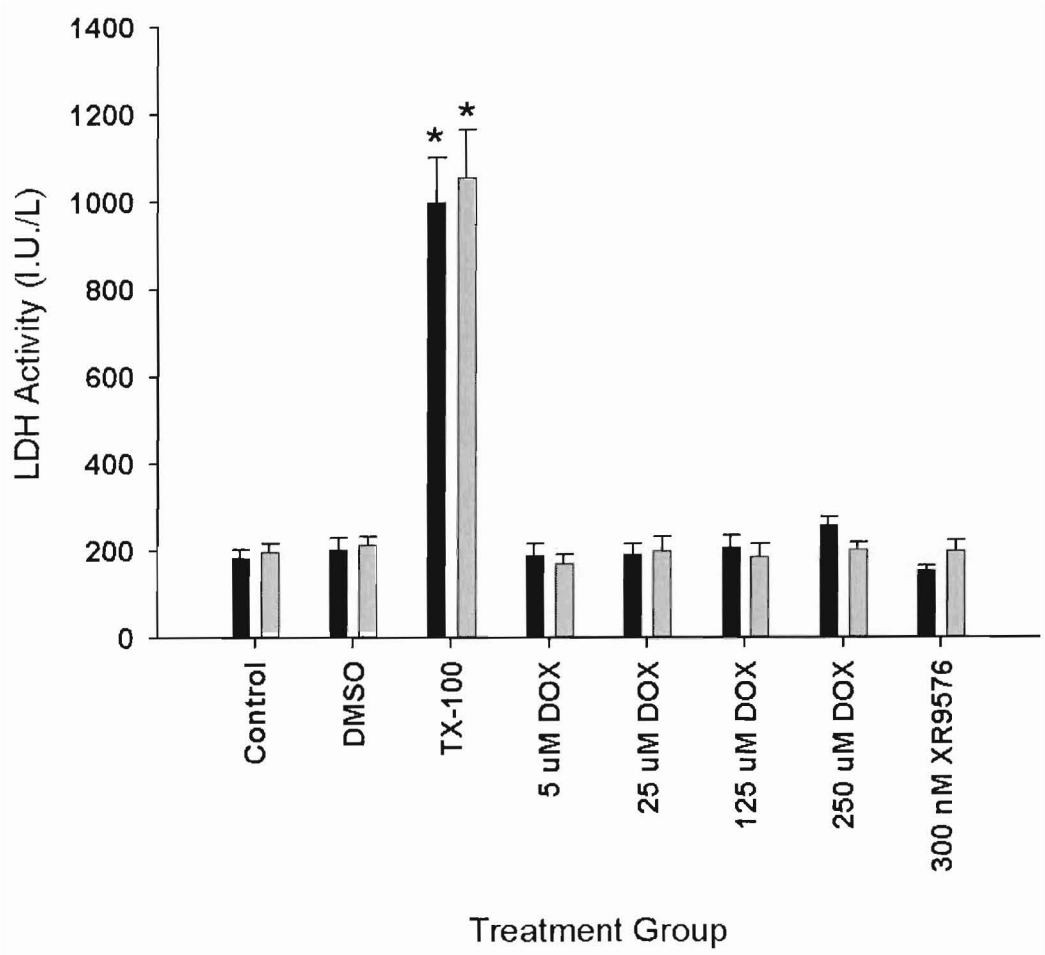
1400
1200
1000
800
600
400
200
0
LDH Activity (I.U./L)
*
*
Control
DMSO
TX-100
5 uM DOX
25 uM DOX
125 uM DOX
250 uM DOX
300 nM XR9576
Treatment Group

concentrations (5, 25, 75, or 125 μM), the accumulation of DOX was linear for approximately 15 min, after which accumulation levelled off (Fig. 4) and steady state was assumed. Initial accumulation rates of DOX by trout hepatocytes incubated with DOX were calculated from linear regressions through the linear portion of each curve (0-5 min).

Calculated initial rates of DOX accumulation were 3.76 ± 0.41, 8.86 ± 1.74, 23.52 ± 1.43, 35.98 ± 4.93 μg/min/10^6 cells for 5, 25, 75, and 125 μM treatments respectively (Figure 5). Rates were all significantly different from each other ($p<0.0001$) except for the following treatments: 5 μM and 25 μM DOX. Rates were concentration dependent (Figure 5).

To characterize P-gp mediated efflux of DOX, hepatocytes were first incubated for 60 min in medium containing various concentrations of doxorubicin, which allowed accumulation to level off (i.e. cells were 'pre-loaded with DOX). Following incubation, hepatocytes were supplied with DOX-free medium (Sturm et al., 2001) and incubated for up to 120 min (Figure 6). Initial efflux of DOX from hepatocytes was fast which was followed by a slower phase where it appeared to level off. Initial efflux rates of DOX were calculated by fitting linear regressions through the linear portion of each curve (0-10min). Calculated initial rates of DOX efflux were 3.57 ± 0.91, 14.89 ± 1.17, 24.02 ± 1.45, 39.17 ± 3.43 μg/min/10^6 cells for the 5, 25, 75, and 125 μM treatments respectively (Figure 7). All treatments were significantly different from each other at $P<0.0001$, and were concentration dependent.

Inhibition of P-gp mediated DOX transport during the efflux phase, was accomplished in this study by using the non-competitive P-gp inhibitor XR9576, which has previously been shown to significantly inhibit P-gp in the drug resistant tumor cell line NCI/ADR^{Res} (Walker *et al.*, 2004). Hepatocytes were incubated for 60 min with DOX and XR9576 for 60, which 'pre-loaded' the cells with DOX. As before, hepatocytes were washed and supplied with doxorubicin/XR9576-free medium and incubated for up to 120 min. Final intracellular concentrations of DOX for the treated and untreated XR9576 treatment groups following a 120 min efflux phase were compared to quantify the amount of P-gp inhibition that had occurred (Figure 8). All treatments showed significantly higher intracellular DOX concentrations when they were treated with XR9576 at 300 nM ($p<0.001$) as compared to the XR9576-untreated groups, except the 5 μM. Intracellular DOX concentrations decreased by 57, 61, 50, and 23 % for the 125, 75, 25, and 5 μM DOX-treated groups. Significant differences for each DOX treatment group from the XR9576 treated groups are represented in the figure with an asterix.

Figure 4. Time course of intracellular DOX accumulation by trout hepatocytes incubated at 5 (●), 25 (O), 75 (▼) and 125 μM (▽). At all concentrations, the accumulation of DOX was linear for approximately 15 min, after which accumulation became saturated and steady state was assumed. Values are means ± SEM., *n*=7.

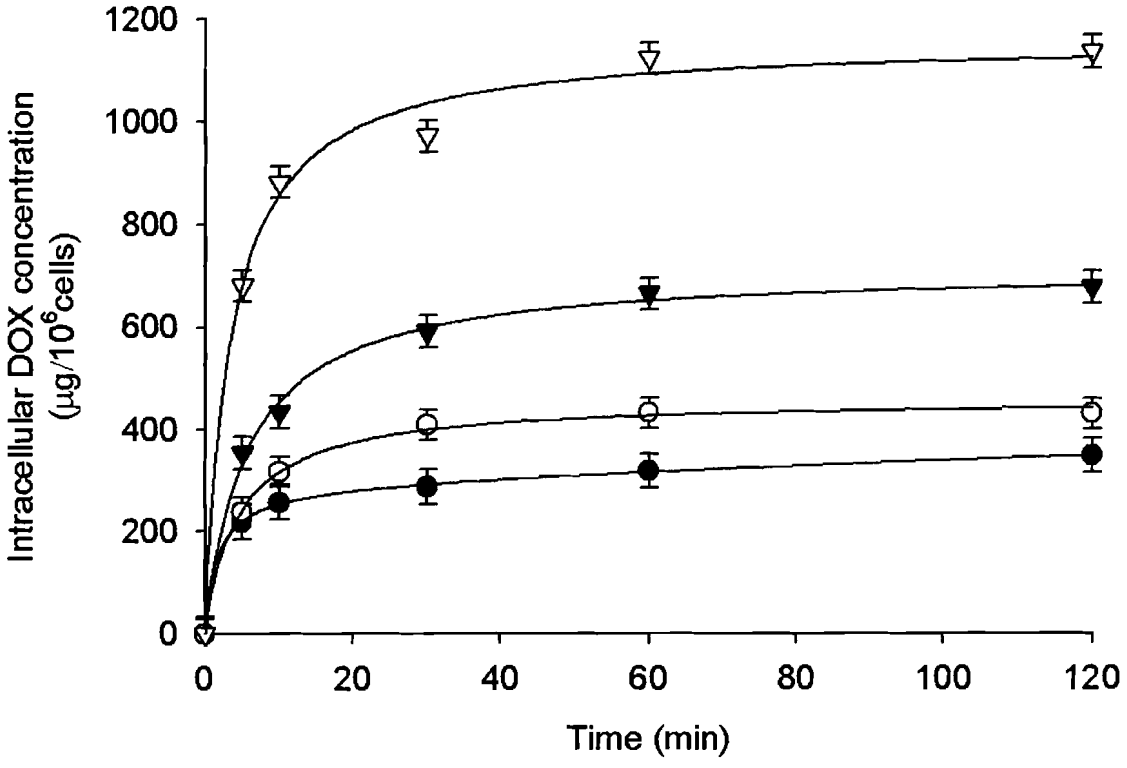
Intracellular DOX concentration
(μg/10^6cells)
1200
1000
800
600
400
200
0
0
20
40
60
80
100
120
Time (min)

Figure 5. Initial accumulation rates of DOX by trout hepatocytes incubated with 5, 25, 75, or 125 μM DOX. Rates were all significantly different from each other ($p<0.0001$), except the 5 and 25 μM treatments. Treatments marked with * are not significantly different from each other. Values are means ± SEM., $n=7$.

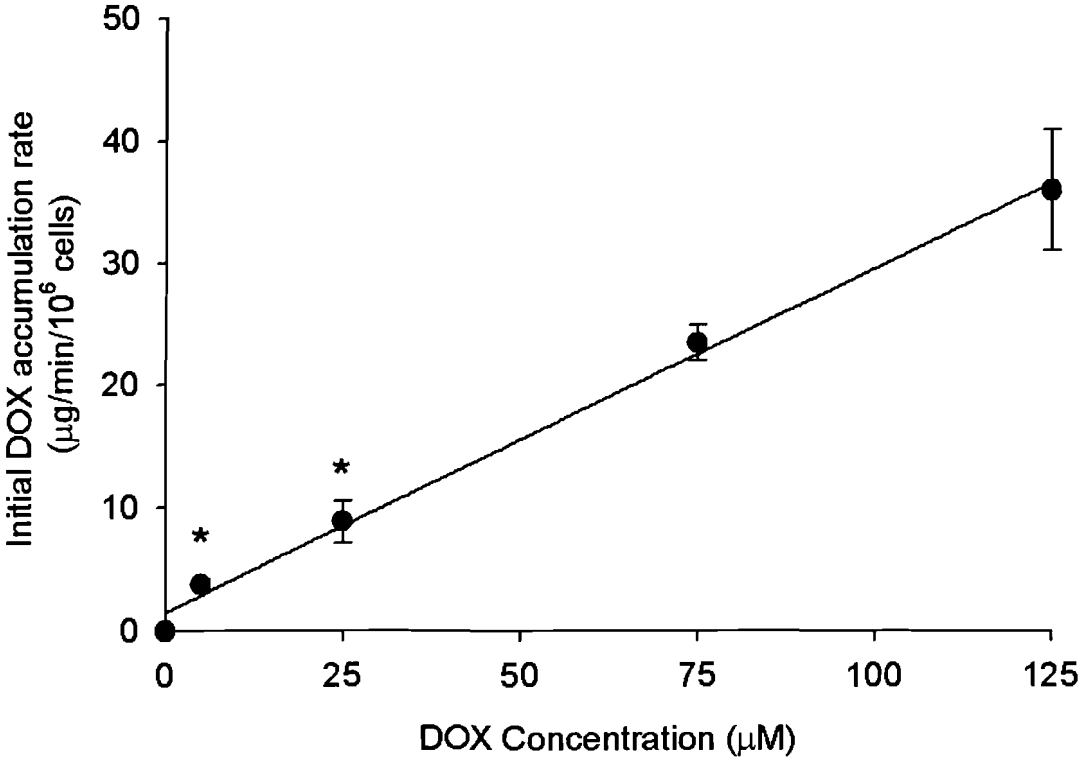
Initial DOX accumulation rate
(μg/min/10^6 cells)
50
40
30
20
10
0
0
25
50
75
100
125
DOX Concentration (μM)
*
*

Figure 6. Time course of DOX efflux by trout hepatocytes following a 60 min incubation with DOX at 5 (●), 25 (○), 75 (▼) and 125 (▽) μM DOX. Values are means ± SEM., *n*=7.

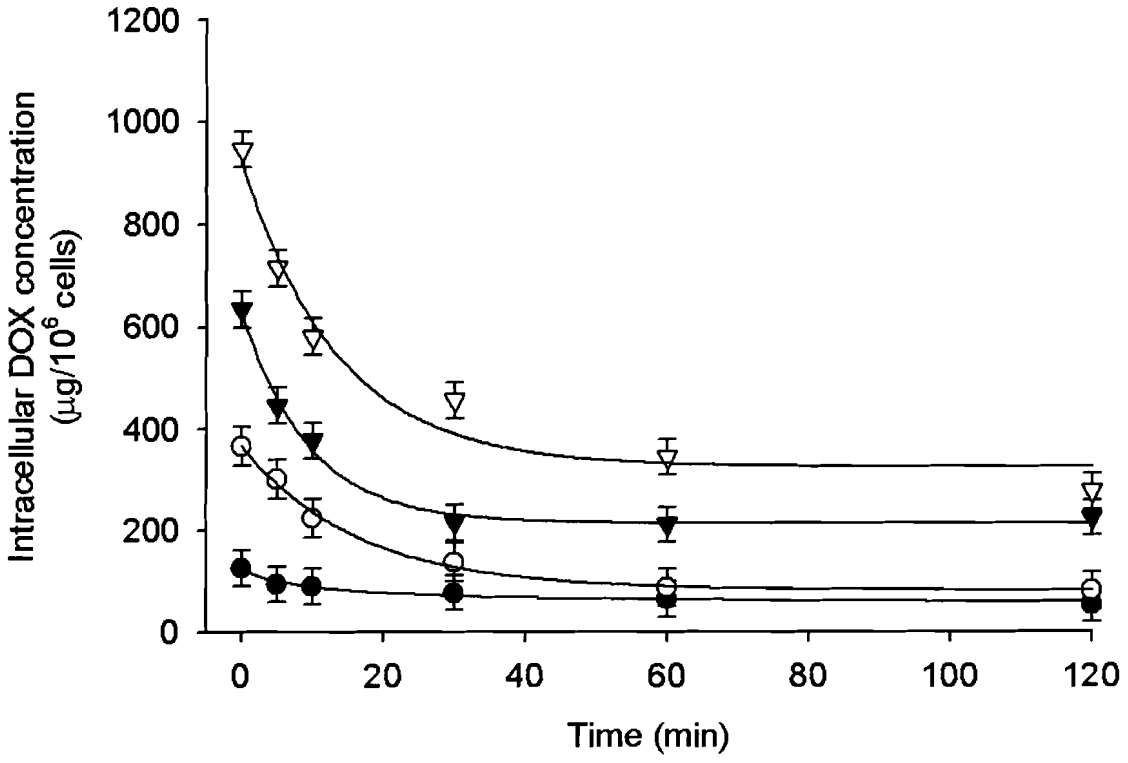
Intracellular DOX concentration
(μg/10^6 cells)
1200
1000
800
600
400
200
0
0
20
40
60
80
100
120
Time (min)

Figure 7. Initial efflux rates of DOX following the pre-incubation of hepatocytes with 5, 25, 75, or 125 μM DOX for 60 min. All treatments were significantly different from each other at $P<0.0001$. Values are means $\pm$ SEM., $n=7$.

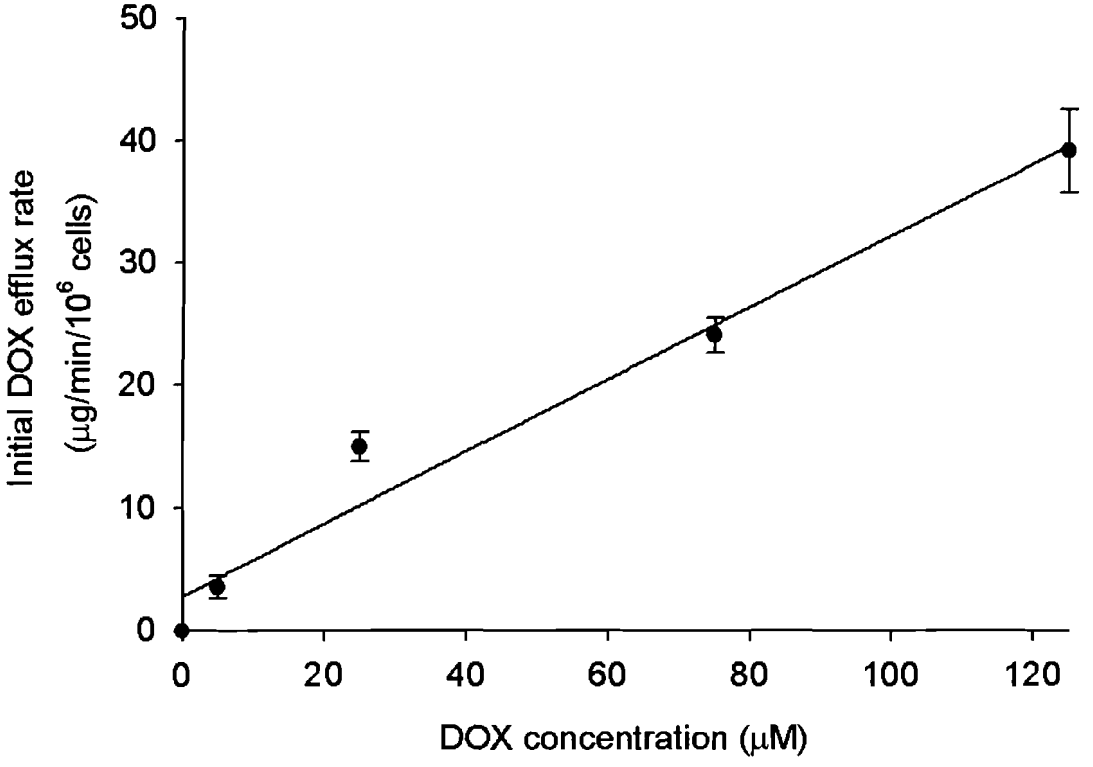
Initial DOX efflux rate
(μg/min/10^6 cells)
50
40
30
20
10
0
0
20
40
60
80
100
120
DOX concentration (μM)

3.3 Adenylate nucleotides

Intracellular ATP, ADP and AMP concentrations from isolated hepatocytes were measured at various time points during the accumulation and efflux phase of P-gp mediated DOX transport and subsequently examined for changes with time, and to determine if differences between treatments existed (Figures 9, 10, 11, and 12).

Hepatocytes were incubated for 60 min with DOX alone, or with both DOX and XR9576 as described previously until steady state was reached. Following this accumulation phase, hepatocytes were supplied with DOX/XR9576-free medium and allowed to efflux for up to 120 min post accumulation. At various time points throughout the accumulation phase (0, 10, 20, 40 and 60 min) and the efflux phase (70, 80, 100, 130, and 190 min), cells were sampled and the intracellular concentrations of ATP, ADP and AMP were measured as previously described.

Figure 8. Intracellular DOX concentrations after incubation of cells for 120 min post accumulation (efflux) for both XR9576-treated (300 nM, ■) and untreated (▨) groups. Significantly higher DOX concentrations were found for all XR9576-treated compared to XR9576-untreated groups, except the 5 μM DOX treatment group. Percent decreases in intracellular DOX concentrations were 57, 61, 50, and 23 % for the 125, 75, 25, and 5 μM DOX-treated groups respectively. Significant differences ($p<0.001$) are marked with *. Values are means ± SEM., *n=7.*

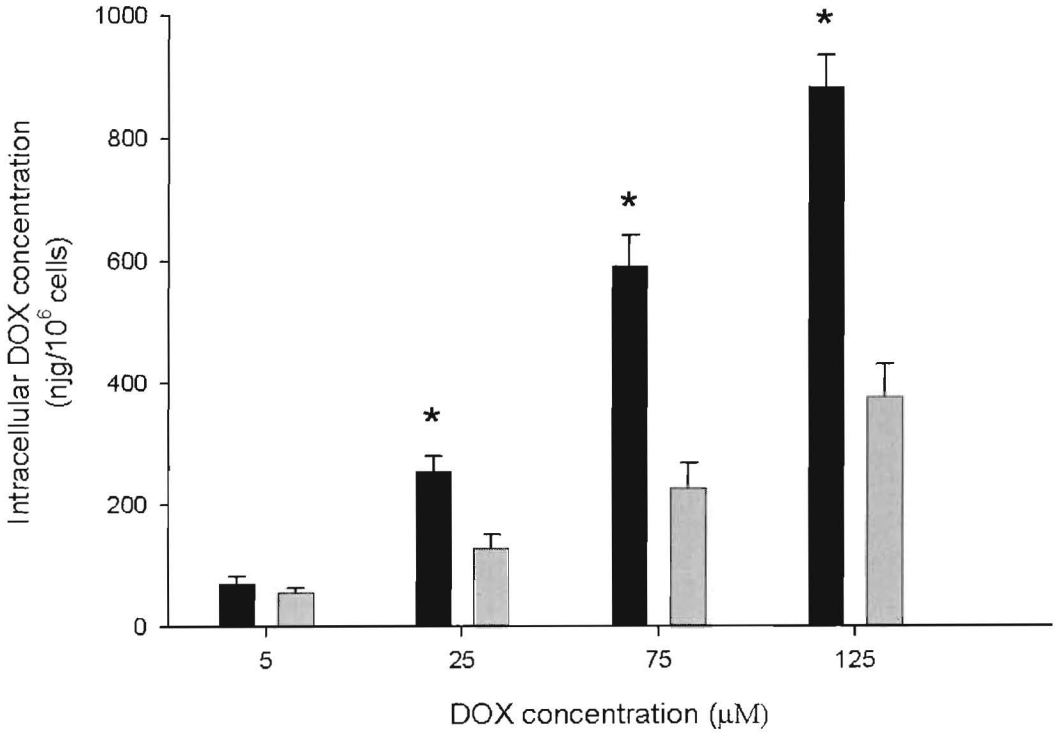
1000
800
600
400
200
0
Intracellular DOX concentration
(njg/10^6 cells)
*
*
*
5
25
75
125
DOX concentration (μM)

Figure 9. Time course of intracellular ATP concentrations (nmol/mg cells) in cells treated with 0 μM DOX (○), 125 μM DOX (●) and 125 μM DOX + 300 nM XR9576 (▼). Intracellular ATP concentrations were compared between time points only for different treatment groups (0 μM DOX, 125 μM DOX, 125 μM DOX + 300 nM XR9576). Symbols with different letters are significantly different from each other ($p<0.001$). Values were also compared amongst treatment groups to find the time at which a significant difference from time zero (baseline) was observed. Symbols with * are significantly different from time zero.

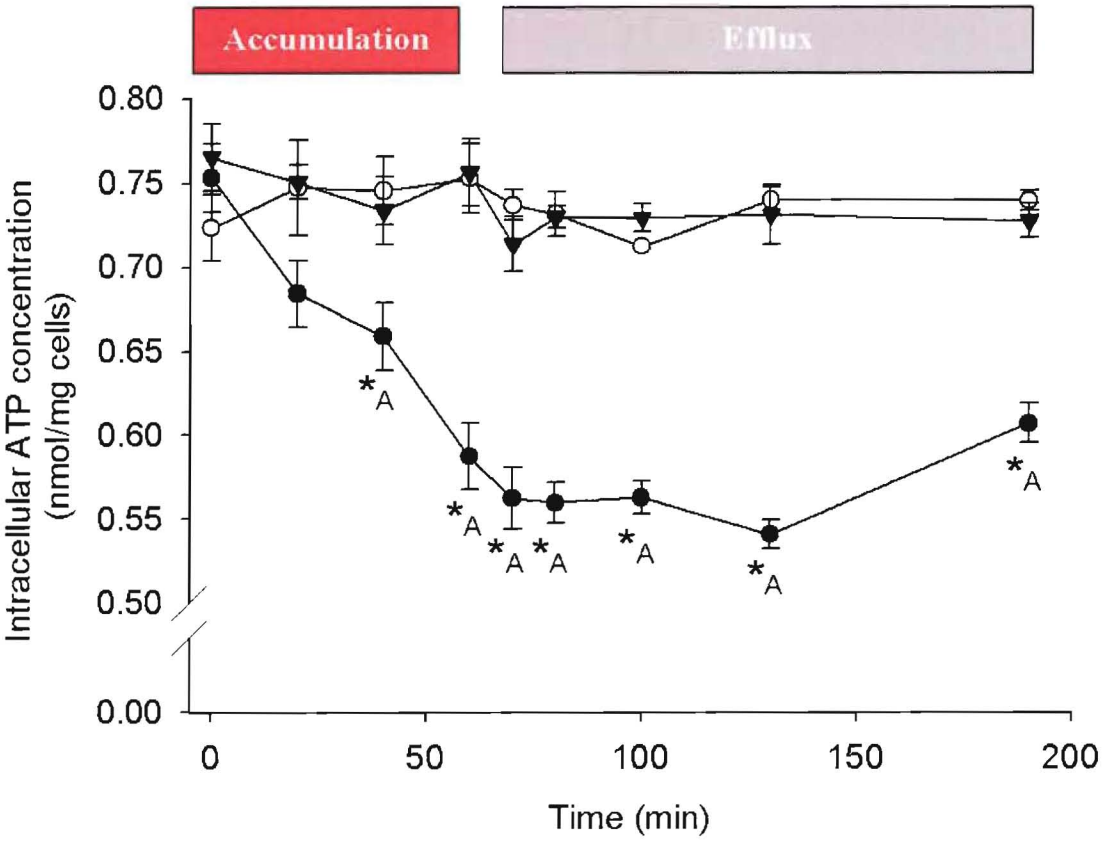
Accumulation
Efflux
Intracellular ATP concentration (nmol/mg cells)
0.80
0.75
0.70
0.65
0.60
0.55
0.50
0.00
0
50
100
150
200
Time (min)
*A

Figure 10. Time course of intracellular ADP concentrations (nmol/mg cells) in cells treated with 0 μM DOX (○), 125 μM DOX (●) and 125 μM DOX + 300 nM XR9576 (▼). Intracellular ADP concentrations were compared between time points only for different treatment groups (0 μM DOX, 125 μM DOX, 125 μM DOX + 300 nM XR9576). Symbols with different letters are significantly different from each other ($p<0.001$). Values were also compared amongst treatment groups to find the time at which a significant difference from time zero (baseline) was observed. Symbols with * are significantly different from time zero.

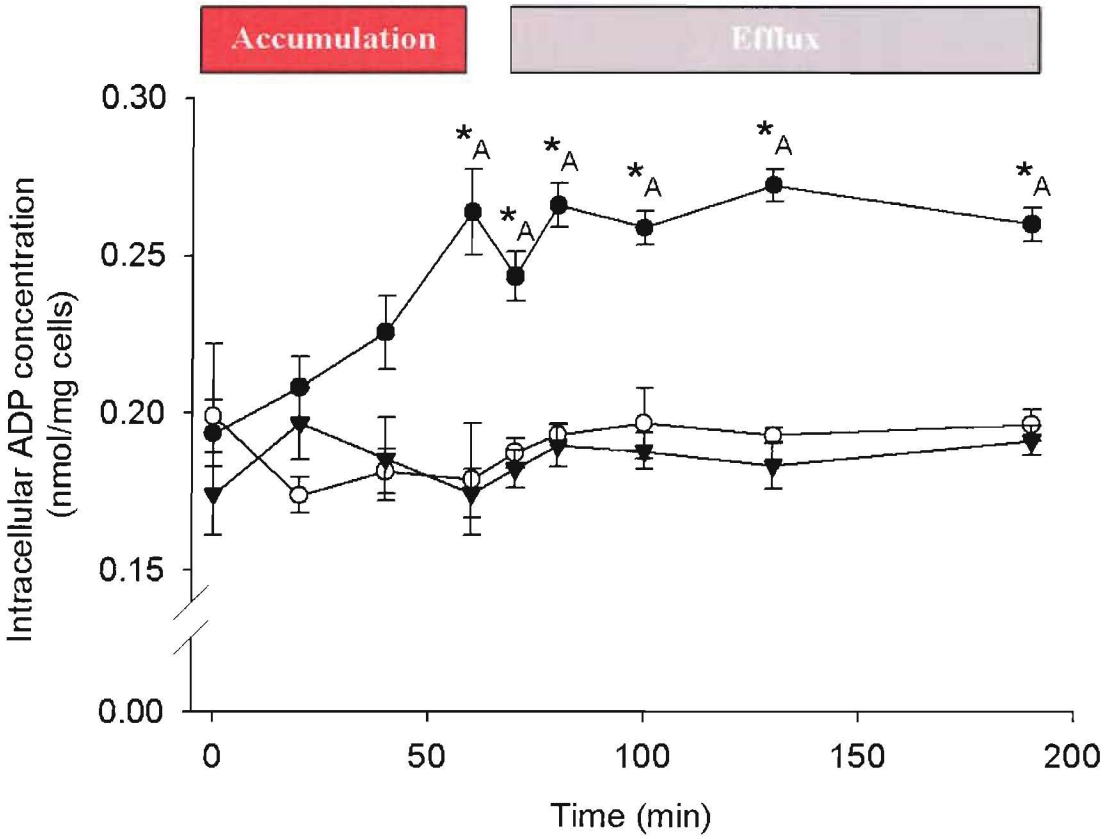
Accumulation
Efflux
Intracellular ADP concentration (nmol/mg cells)
0.30
0.25
0.20
0.15
0.00
*A
*A
*A
*A
*A
*A
0
50
100
150
200
Time (min)

Figure 11. Time course of intracellular AMP concentrations (nmol/mg cells) for 0 μM DOX (O), 125 μM DOX (●) and 125 μM DOX + 300 nM XR9576 (▼). Values were compared between time points only for different treatment groups (0 μM DOX, 125 μM DOX, 125 μM DOX + 300 nM XR9576). Symbols with different letters are significantly different from each other ($p < 0.001$). Intracellular AMP concentrations were also compared amongst treatment groups to find the time at which a significant difference from time zero (baseline) was observed. Symbols with * are significantly different from time zero.

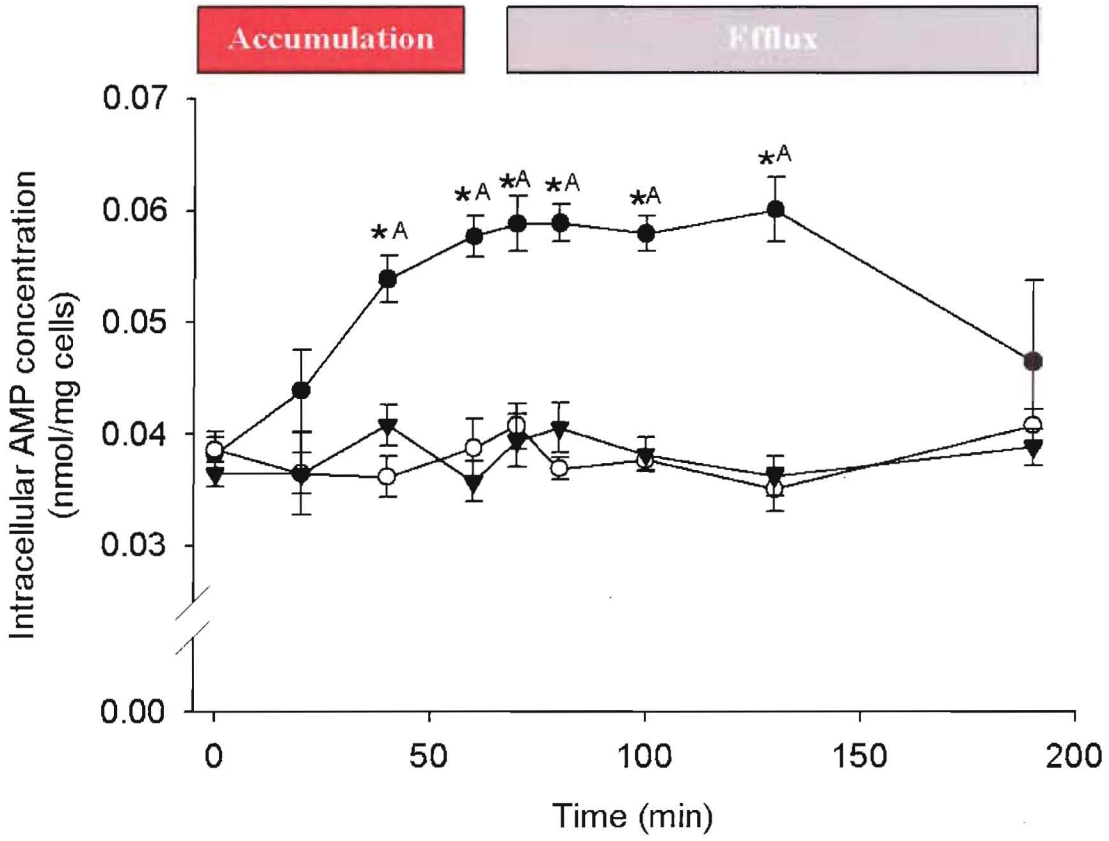
Accumulation
Efflux
Intracellular AMP concentration (nmol/mg cells)
0.07
0.06
0.05
0.04
0.03
0.00
*A
*A
*A
*A
*A
*A
0
50
100
150
200
Time (min)

Figure 12. Time course of intracellular inorganic phosphate (Pi) concentrations (nmol/mg cells) for (○), 125 μM DOX (●) and 125 μM DOX + 300 nM XR9576 (▼). Values were compared between time points only for different treatment groups (0 μM DOX, 125 μM DOX, 125 μM DOX + 300 nM XR9576). Symbols with different letters are significantly different from each other ($p<0.001$). Values were also compared amongst treatment groups to find the time at which a significant difference from time zero (baseline) was observed. Symbols with * are significantly different from time zero.

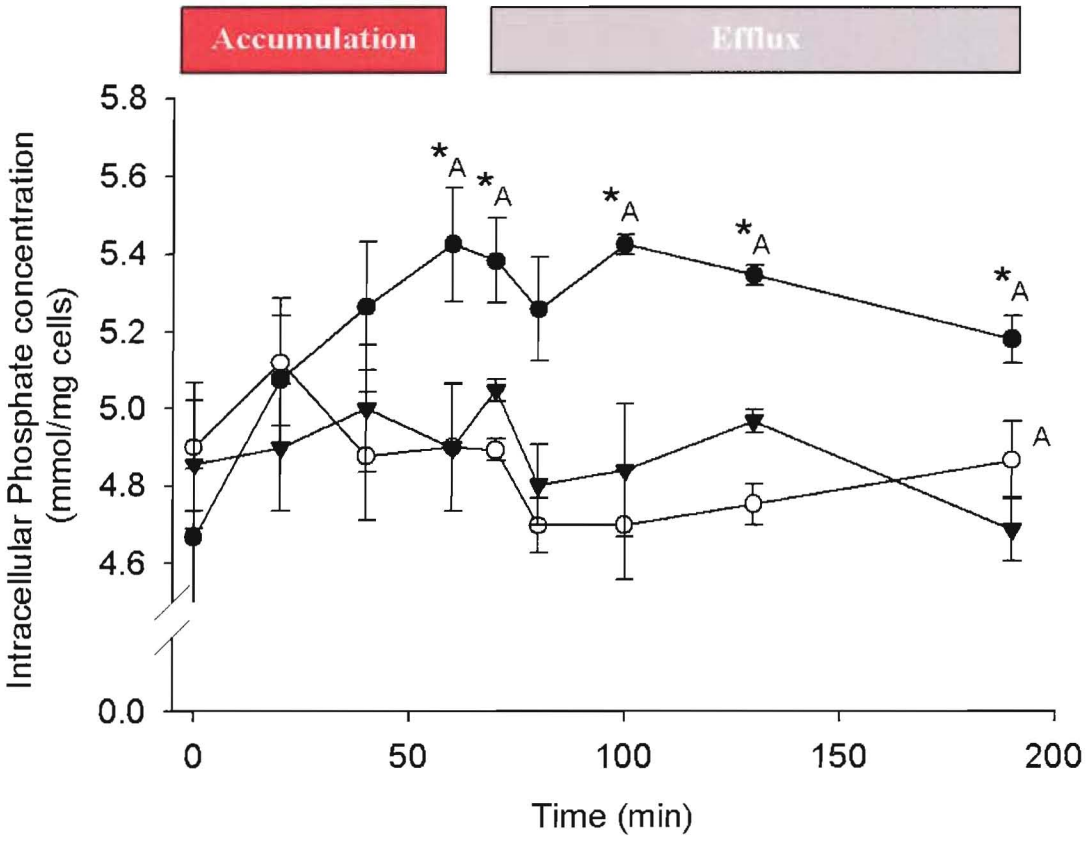
Accumulation
Efflux
Intracellular Phosphate concentration (mmol/mg cells)
5.8
5.6
5.4
5.2
5.0
4.8
4.6
0.0
0
50
100
150
200
Time (min)
*A
*A
*A
*A
*A
A

3.3.1 ATP concentrations

Intracellular ATP concentrations were measured in hepatocytes exposed to 125 μM DOX as well as one treatment group exposed to both 125 μM DOX and 300 nM XR9576 together. During the accumulation phase of the exposure, no significant difference was seen in ATP concentration with time between control and the DOX/XR9576 group (Figure 9). Similarly, no difference between controls and the DOX/XR9576 group were seen in intracellular ATP concentration during the compound efflux phase (Figure 9). When cells were exposed to DOX alone, significant decreases ($p<0.001$) in intracellular ATP concentrations were seen at 40 min post-incubation during the accumulation phase which persisted through the efflux phase (Figure 9). The lowest ATP concentration was observed at 130 min post-incubation during the efflux phase with a percent decrease of 25% from baseline.

3.3.2 ADP concentrations

Intracellular ADP concentrations were measured in hepatocytes as described above for ATP. During the accumulation phase of the exposure, no significant difference was seen in ADP concentration with time between control and the DOX/XR9576 group (Figure 10). Similarly, no difference between controls and the DOX/XR9576 group were seen in intracellular ADP concentration during the compound efflux phase (Figure 10). When cells were exposed to doxorubicin alone, significant increases ($p<0.001$) in intracellular ADP concentrations were seen at 60 min post incubation during the accumulation

phase and persisted through the efflux phase (Figure 10). The highest ADP concentration was observed at 130 min post-incubation during the efflux phase with a percent increase of 26% from baseline.

3.3.3 AMP concentrations

Intracellular ADP concentrations were measured in hepatocytes as described above for ATP. During the accumulation phase of the exposure, no significant difference was seen in AMP concentration with time between control and the DOX/XR9576 group (Figure 11). Similarly, no difference between controls and the DOX/XR9576 group were seen in intracellular AMP concentration during the compound efflux phase (Figure 11). When cells were exposed to doxorubicin alone, significant increases ($p<0.001$) in intracellular AMP concentrations were seen at 40 min post incubation during the accumulation phase and persisted through the efflux phase until 130 min (Figure 11). The highest AMP concentration was observed at 130 min post-incubation during the efflux phase with a percent increase of 36% from baseline.

3.3.4 Inorganic phosphate

Intracellular inorganic phosphate (Pi) concentrations were measured in hepatocytes as described above for ATP. During the accumulation phase of the exposure, no significant difference was seen in Pi concentration with time between control and the DOX/XR9576 group (Figure 12). Similarly, no difference between controls and the DOX/XR9576 group were seen in intracellular Pi

concentration during the compound efflux phase (Figure 12). When cells were exposed to DOX alone, significant inc ($p<0.001$) increases intracellular Pi concentrations were seen at 60 min post incubation during the accumulation phase and persisted through the efflux phase (Figure 12). The highest percent increase (11%) from baseline in Pi was observed at 100 min post-incubation during the efflux phase.

3.4 Adenylate energy charge and phosphorylation potential

Adenylate energy charge (AEC) and phosphorylation potential (PP) were calculated from measured intracellular concentrations of ATP, ADP, AMP, Pi, and subsequently examined for changes with time, or to determine if differences existed between treatment groups (Figures 13, and 14).

AEC was calculated from measured ATP, ADP and AMP in hepatocytes as described above for ATP. During the accumulation phase of the exposure, no significant difference was seen in AEC with time between control and the DOX/XR9576 group (Figure 13). Similarly, no difference between controls and the DOX/XR9576 group were seen in AEC during the compound efflux phase (Figure 13). When cells were exposed to doxorubicin alone, significant decreases ($p<0.001$) in AEC were seen at 60 min and persisted through the efflux phase (Figure 13). The lowest AEC occurred at 130 min post-incubation during the efflux phase with a percent decrease of 11% from baseline.

Figure 13. Time course of adenylate energy charge (AEC) in isolated rainbow trout hepatocytes for 0 µM DOX (O), 125 µM DOX (●) and 125 µM DOX + 300 nM XR9576 (▼). Symbols with different letters are significantly different from each other ($\alpha < 0.05$). Values were also compared amongst treatment groups to find the time at which a significant difference from time zero (baseline) was observed. Symbols with * are significantly different from time zero.

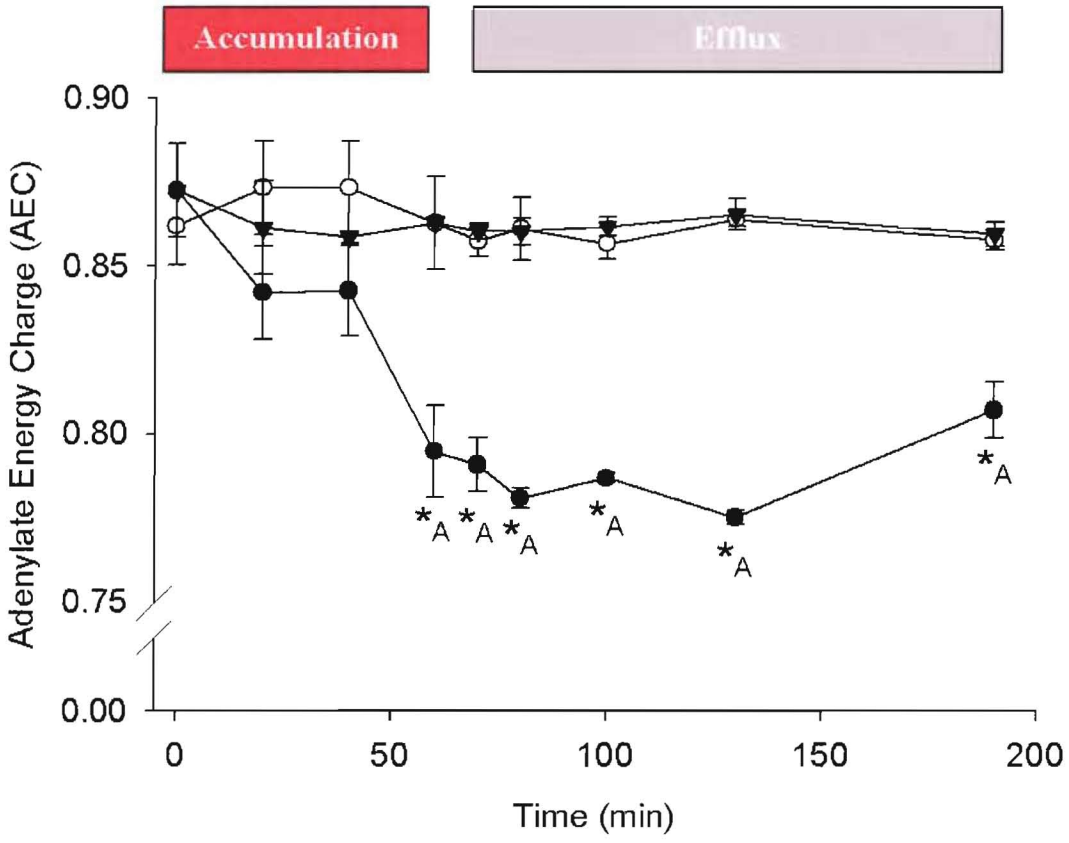
Accumulation
Efflux
0.90
0.85
0.80
0.75
0.00
Adenylate Energy Charge (AEC)
*A
*A
*A
*A
*A
*A
0
50
100
150
200
Time (min)

Figure 14. Time course of the phosphorylation potential in isolated rainbow trout hepatocytes for 0 µM DOX (O), 125 µM DOX (●) and 125 µM DOX + 300 nM XR9576 (▼). Symbols with different letters are significantly different from each other ($\alpha < 0.05$). Values were also compared amongst treatment groups to find the time at which a significant difference from time zero (baseline) was observed. Symbols with * are significantly different from time zero.

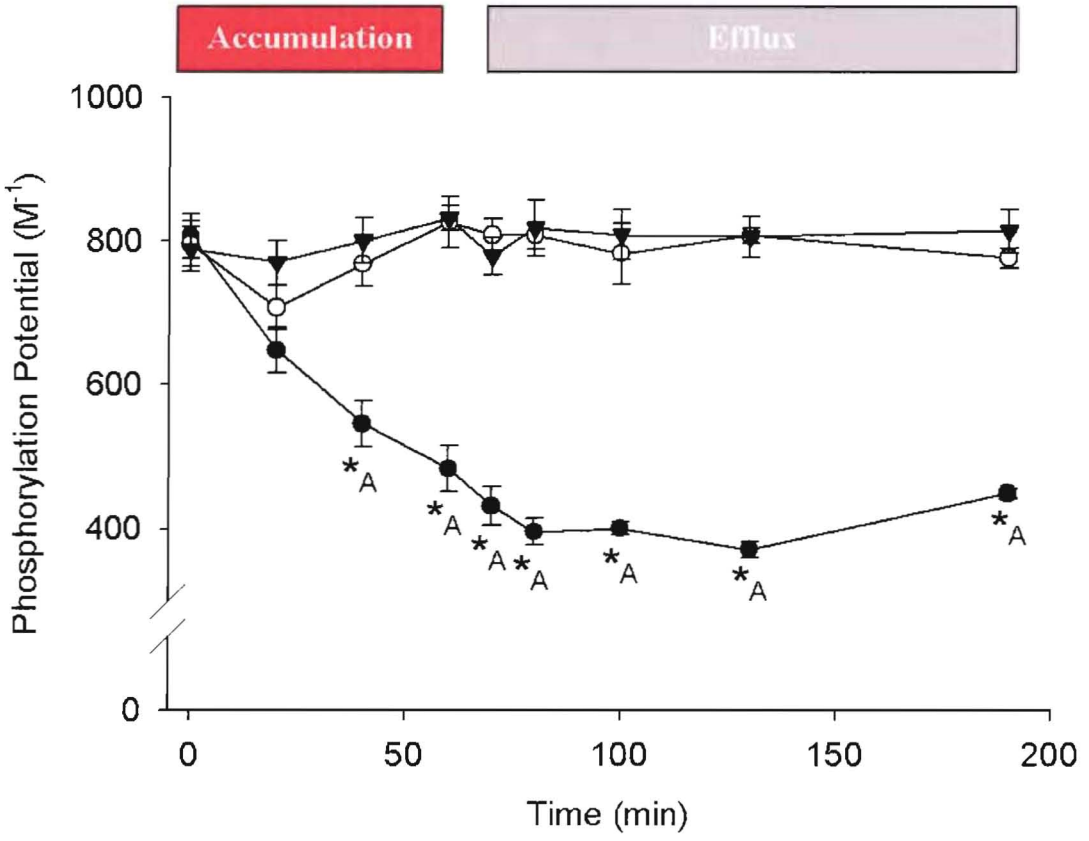
Accumulation
Efflux
1000
800
600
400
0
Phosphorylation Potential (M^{-1})
0
50
100
150
200
Time (min)
*A
*A
*A
*A
*A
*A
*A

PP was calculated from measured ATP, ADP and AMP and Pi in hepatocytes as described above for ATP. During the accumulation phase of the exposure, no significant difference was seen in PP with time between control and the DOX/XR9576 group (Figure 14). Similarly, no difference between controls and the DOX/XR9576 group were seen in PP during the compound efflux phase (Figure 14). When cells were exposed to DOX alone, significant decreases ($p<0.001$) in PP were seen at 60 min post incubation during the accumulation phase and persisted through the efflux phase (Figure 14). The lowest PP was observed at 130 min post-incubation during the efflux phase with a percent decrease of 53% from baseline.

4.0 DISCUSSION

In dealing with environmental contaminants, organisms have developed cellular defense mechanisms to protect themselves against pollutant exposure. These same defense mechanisms which protect organisms against xenobiotic exposure are likely to also have energetic and metabolic costs associated with their maintenance, regulation and activity, which may in turn have negative impacts on an organism's overall energy budget. These costs may affect energy budgets when energy is limiting, by causing a reallocation of energy expenditures, (in order to maintain a balance between energy gained and energy lost). Such a reallocation of energy expenditures may be in the form of a decrease in energy allocations to growth or reproduction (Brett and Groves, 1979; Kitchell, 1983) which could ultimately affect fitness. Studies have examined energetic costs of cellular defense mechanisms by studying effects at the cellular and biochemical level; however, most studies have not been able to assess energetic costs associated with detoxification without also taking into account toxic effects which may affect energy use. Recently, work with trout hepatocytes has examined respiratory costs of pyrene exposure and biotransformation (Bains and Kennedy, 2004) and respiratory costs associated with P-glycoprotein (P-gp) transport activity of Rhodamine 123 (R123) (Bains and Kenndy, 2005). The aim of the current study was to further characterize the

functional activity of P-gp, and specifically, to assess the energetic costs associated with its activity in the transport of the P-gp substrate doxorubicin (DOX).

4.1 Hepatocytes as a model system

In the past two decades there has been an increased interest in the use of aquatic organisms as model systems for toxicological research and as monitors of chemical pollution (Malins, 1991), and a shift in research to study the effects of chemicals on cellular and sub-cellular systems. Studying such lower level, *in vitro* effects has several advantages over *in vivo* systems, particularly in identifying mechanisms of action for cause-effect relationships; however results from *in vitro* studies can be difficult to extrapolate to higher-level whole organism effects, and may lack ecological relevance.

Additional advantages of *in vitro* systems include the ability to control environmental conditions and eliminate interactive systemic effects, reduce variability between experiments, the generation of smaller quantities of toxic wastes, and simultaneous or repeated sampling over time (Baksi and Frazier, 1990).

The use of mammalian hepatocytes over the past 20 years in toxicological research has become well established, and more recently, fish hepatocytes have become model systems for studying toxic effects on cellular and sub-cellular systems and for monitoring chemical pollution. Fish hepatocytes have been

used in physiological and biochemical studies including energy metabolism (Seibert, 1985a; Simon 1985), nitrogen metabolism (Casey et al., 1983), intracellar pH regulation (Walsh and Moon, 1983), carbohydrate metabolism (Mommsen, 1986), protein synthesis (Koban, 1987), and lipid metabolism (Hazel, 1982). Fish hepatocytes have also been used in toxicological research including cytotoxicity studies (Gagné and Blaise, 1999, 2001), carcinogenicity and genotoxicity studies (Klaurıig, J.E., 1984; Gagné and Blaise, 1999; Risso-de Faverney et al., 2001), studies on xenobiotic metabolism (Pesonen and Anderson, 1997; Bains and Kennedy, 2004), and more recently toxicogenomics (Finne et. al, 2007).

The isolation of fish hepatocytes for studying toxicological effects of chemicals has become a well established procedure and their use in toxicological studies involving detoxification and P-gp transport is increasing. Recent studies in trout hepatocytes have examined energetic costs associated with xenobiotic induced P-gp transport activity (Bains and Kennedy, 2004, 2005). Therefore, the use of hepatocytes was considered a good system in this study.

4.2 Cell viability and cytotoxicity

In order to determine if hepatocytes were damaged by chemical exposure to the P-gp substrate DOX and P-gp inhibitor tariquidar (XR9576), respectively, cell viability and membrane integrity were measured by trypan blue exclusion, and LDH leakage. Maintenance of functionally intact cells is important when examining P-gp transport activity and when calculating adenylate parameters as

an indicator of cellular energy state. Cell viability was assessed by Trypan Blue exclusion, and ranged between 81.8 and 88.8% during the isolation and chemical exposure period. These results are similar to those of studies in fish. For example, in trout hepatocytes, cell viabilities were found to be greater than 87% (Bains and Kennedy, 2004) and greater than 87% (Bains and Kennedy, 2005), following isolation procedures outlined in this study.

No significant differences in LDH release from hepatocytes incubated with DOX and/or XR9576 were found when compared to controls. The LDH activity of the DOX and/or XR9576-treated hepatocytes was found to be significantly lower (154.6 ± 9.6 to 258.3 ± 19.2 IU/L) than the TX-100 group (999.5 ± 100.9 to 1056.2 ± 110.2). These results indicate that neither doxorubicin nor XR9576 caused damaged to hepatocytes at the exposure concentrations used. Therefore, DOX and XR9576 were considered to be excellent model compounds for use in this study.

4.3 Accumulation and Efflux of Doxorubicin

In order to correlate changes in adenylate parameters and phosphorylation potential (PP) to P-gp activity, a functional characterization of P-gp mediated DOX transport was necessary.

The expression of P-gp in various organs in several fish species has been confirmed by several studies (Hemmer, 1995; Kleinow, 2000; Bard, 2002), and its activity has been functionally characterized in rainbow trout hepatocytes (Sturm, 2001; Bains and Kenndy, 2005). In 2001, it was confirmed by Sturm et

al., that the transport activity of R123 and was not due to Multidrug-resistance proteins (MRPs) but rather to mdr 1-type P-gp mediated activity.

In the present study, accumulation and efflux assays in trout hepatocytes were carried out following similar protocols to previous studies (Bains and Kennedy, 2005; Sturm, 2001). Accumulation of DOX appeared linear for approximately 60 min after which steady state was assumed. Initial accumulation rates calculated from the linear portion of the curve increased in a linear fashion DOX concentration. These results are similar to those of Sturm et al., (2001), and Albertus and Laine, (2001). DOX is known to enter cells via passive diffusion (Hilmer, 2004), and the major route of excretion has been shown to be via biliary excretion by P-gp, with a small fraction metabolized to doxorubicinol (Ballet et al., 1987; Booth et al., 1996). During the initial accumulation phase, from which accumulation rates were calculated, it is likely that DOX was also being actively transported out of the cell via P-gp. Therefore, the calculated initial rates of accumulation are not a direct measurement of DOX influx. The purpose of the accumulation experiments was to determine the point at which steady state was reached allowing for the maximization of pre-loading values prior to the compound efflux phase. The results for the initial accumulation of DOX in this study are similar to those found by Sturm et al, (2001) for DOX accumulation by P-gp, however in comparison to R123 accumulation, the initial DOX accumulation in this study appeared to be faster than in previous studies (Sturm et al., 2001; Bains and Kenndy, 2005).

P-gp mediated efflux of DOX and the calculation of initial efflux rates followed protocols of two previous studies (Bains and Kennedy, 2005; Sturm, 2001). Initial efflux rates were calculated by fitting a linear regression through the linear portion of each curve, and results indicated that initial efflux rates increased with DOX exposure in a concentration dependent manner as was found in other studies with DOX (Sturm et al, 2001) and R123 (Sturm et al., 2001; Bains and Kennedy, 2005). The calculated initial rates of DOX efflux in this study are faster than those found for R123 efflux from trout hepatocytes (Sturm et al., 2001, Bains and Kennedy, 2005).

In this study, P-gp mediated transport of DOX was inhibited by the, non-competitive inhibitor XR9576. XR9576 has been shown to completely reverse the resistance of P-gp expressing cell lines to a wide range of cytotoxic agents including colchicine, doxorubicin, and vinblastine (Stewart et al., 1998; Mistry et al.,2001; Walker et al., 2004). The non-competitive nature of XR9576 was examined in chinese hamster ovary parental ($CH^{r}B30$) cells where it was shown to be a potent inhibitor of P-gp mediated vinblastine and paclitaxel transport (Martin et al., 1999). The study by Martin et al., (1999) suggests a non-competitive interaction between XR9576 and the P-gp substrates vinblastine and paclitaxel. XR9576 has also been used as an inhibitor of P-gp mediated R123 transport in trout hepatocytes (Bains and Kennedy, 2005). These authors were also able to attribute increased cellular respiratory rates to P-gp transport activity and not other potential cellular effects of R123. Similarly, XR9576 was used in

this study to inhibit P-gp mediated DOX transport in order to attribute any changes in adenylate parameters to P-gp transport activity, alone.

In this study, XR9576 at a concentration of 300 nM was found to significantly reduce DOX efflux in hepatocytes exposed to 125, 75, and 25 μM DOX following a 2-h incubation period. Percent differences of intracellular DOX between XR9576-treated and un-treated hepatocytes were 57%, 61%, and 50% for the 125, 75, and 25 μM treatments respectively. No significant difference (23%) in intracellular DOX was found between XR9576-treated and un-treated hepatocytes exposed to 5 μM DOX. These results are similar to those of Bains and Kennedy (2005) who showed that at 300 ηM, XR9576 was able to reduce R123 efflux by 42% following a 2-h incubation. The inability of XR9576 to completely inhibit P-gp transport of DOX in this study may have due to the concentration of XR9576 chosen. It is suggested that perhaps in order to achieve complete inhibition of P-gp transport of DOX in trout hepatocytes, the concentration of XR9576 should be above 300 ηM.

4.4 Adenylate Energy Charge and Phosphorylation Potential

The adenylate energy charge (AEC) is a measure of the degree of phosphorylation of the ATP-ADP-AMP system, and therefore provides an indication of the amount of energy available to an organism from the adenylate pool (Atkinson, 1977). By measuring adenylate parameters such as the intracellular concentrations of ATP, ADP, and AMP, the AEC can be calculated and used as an indicator of cellular energy state in an organism. Another

indicator of cellular energy state is PP (Lehninger, 2005, 1975) which is calculated from measured concentrations of ATP, ADP, AMP, and Pi. It has been suggested that PP varies with the metabolic state of the cell with higher values being indicative of a more highly energized cell (Lehninger, 2005, 1975). However, the use of PP recently as indicator of cellular energy state has not been significant. A study in 2004 examined the effects of hypoxia on cellular energy state in cardiac muscle extracts in the hypoxia tolerant freshwater turtle and the hypoxia sensitive rainbow trout. These authors reported decreases in PP of 94% and 57% in the trout and turtle respectively during a period of severe hypoxia (Overgaard and Gesser, 2004).

The concentration of ATP in intact living cells is normally higher than ADP and AMP, and AEC is therefore close to 1.0. However, when an increase in energetic demand is placed on a cell, energy requirements greatly increase which leads to a sudden decrease in ATP concentration and a subsequent rise in ADP and Pi concentration due to ATP de-phosphorylation. In response, energy yielding processes such as glycolysis and cellular respiration are accelerated to keep up with ATP utilization (Lehninger, 2005, 1975). When the energetic demand is reduced or removed, ATP yielding processes slow down in response to an increase in ATP concentration and a decrease in ADP concentration (Lehninger, 2005, 1975).

Adenylate parameters such as ATP, ADP, and AMP concentrations, as well as the AEC have been used to measure different types of stress, which may translate in to an increase in energy requirements, in fish including hypoxia

(Vetter and Hodson, 1980), muscular exertion (Driedzic and Hochachka, 1980), low pH (McFarleane, 1981), temperature stress (Walesby and Johnston, 1980) and heavy metal stress (Heath, 1984). In this study, intracellular ATP, ADP, AMP and inorganic phosphate (Pi) were measured during the accumulation and compound efflux phase of P-gp mediated DOX transport to measure energetic costs associated with increased xenobiotic P-gp transport.

This study found that following a 190 min incubation (60 min accumulation + 120 min efflux) of hepatocytes with DOX at a concentration of 125 µM significantly reduced the intracellular concentration of ATP, increased the intracellular concentrations of ADP, AMP and Pi, and decreased the AEC and PP compared to controls and XR9576-treated groups. The highest percent decrease in intracellular ATP concentration was 25% from baseline. Highest percent increases in ADP, AMP, and Pi were 26%, 36%, and 11% respectively. AEC and PP were lowest at 130 min post-incubation with percent decreases from baseline of 11% and 53% respectively, which were maintained through out the 190 min incubation period (i.e. no recovery to baseline values was observed). The lack of recovery of AEC to baseline values is likely due to an increase in the activity level of AMP deaminase, which catalyzes the deamination of AMP to inosine monophosphate (IMP) seen as a decrease in AMP, thus stablilizing the AEC as was observed in previous studies (Matsui et al., 1994; Chapman and Atkinson, 1973). A percent decrease of 11% in AEC correlates to an AEC value of 0.77, which indicates an energetic cost associated with P-gp-mediated transport of DOX. These results indicate that during the accumulation phase, an

increase in energy use was placed on the hepatocytes. This increased energy use caused an increase in ATP utilization resulting in a decrease in ATP concentration and increase in ADP, AMP and Pi concentrations. It is suggested that the increase in energy requirement is likely attributable to the active efflux of DOX out of the cell via P-gp. During the accumulation phase, DOX was entering the cells via passive diffusion; however, it is likely that active transport of DOX out of the cell via P-gp was also occurring at this time since DOX had already begun to accumulate in the cells. This active transport activity of P-gp is powered by the energy derived from ATP hydrolysis from which the products are ADP + Pi during orthophosphate cleavage, and AMP + Pi during pyrophosphate cleavage. ATP-binding cassette (ABC) proteins, such as P-gp, mediate the ATP dependent transport (efflux in the case of P-gp) of a wide range of substrates. P-gp like other ABC transporters, contains two transmembrane domains (TMDs), and two nucleotide binding domains (NBDs) (Higgins, 1992). The P-gp or transport of substrates across biological membranes is highly dependent on energy derived from the coupling of ATP hydrolysis to drug transport (Callaghan, 2005), and involves an allosteric communication between drug binding sites and the two NBDs (van Veen, 2003). The transport process is suggested to occur in 4 stages: 1) loading of P-gp with substrate, 2) switch from high affinity (to promote drug binding) to low affinity (to promote drug dissociation, 3) energy utilization, and 4) re-setting to the basal conformation (Callaghan, 2003). The stoichiometry between drug binding and the amount of ATP hydrolyzed per translocation even

remains debatable, however several studies have reported values between 1 and 3 (Eytan et al., 1996; Ambudkar et al., 1997; Shapiro and Ling, 1998).

The lack of differences between intracellular ATP, ADP, AMP and Pi concentrations in hepatocytes exposed to 125 μM in the presence of XR9576 compared to XR9576-untreated groups indicates that the decrease in AEC and PP representing energy drains, are attributable to P-gp transport activity and not other effects of DOX within the cells. The inability of XR9576 to fully inhibit P-g transport of DOX did not significantly change AEC from controls (i.e. AEC was maintained at control values when P-gp was inhibited by 57%), indicating that the cells were able to maintain energy homeostasis when P-gp was still actively pumping at 43%.

Adenylate parameters such as concentrations of ATP, ADP, and AMP, as well as AEC have been shown to be good measures of energetic costs associated with contaminant exposure in invertebrates (LeBras, 1995), fish (Heath, 1984), insects (Migula, 1997). In 1995, LeBras showed that lindane exposure at concentrations of 4, 8 and 10 μg/L, in whole body extracts of the aquatic invertebrate *Asselus aquaticus* L. caused percent decreases in AEC 10%, 16%, and 6%, which was reported to be indicative of increased energetic and metabolic costs associated with toxicity. Similarly, decreases in AEC of 12% ,19% ,6%, were indicative of energetic costs associated with cadmium toxicity in whole body extracts of red wood ant pupa (Migula, 1997), 96-h copper exposure in liver tissue extracts of the Bluegill (*Lepomis macrochirus*) (Heath, 1984), and

pentachlorophenol exposure in tissue extracts of red abalone foot muscles (Shofer and Tjeerdema, 1998).

All these results indicate that cellular adenylate parameters are good measures of metabolic and energetic costs accrued by organisms during xenobiotic exposure; however, these studies did not examine energetic costs associated detoxification alone, rather they also involved costs of toxicity. The ability to isolate costs associated only with cellular defense, such as increased P-gp transport of xenobiotics without taking into account toxicity effects is important when trying to quantify the energetic costs associated with cellular defense.

AEC has been used as an indicator of cellular energy state during inhibition of metabolic process such as glycolysis, fatty oxidation, and oxidative phosphorylation in cultured rat hepatocytes (Miatsui et al, 1994). These authors reported percent decreases in AEC of 14%, 56%, and 23% after inhibition of fatty acid oxidation, oxidative phosphorylation, and glycolysis respectively over an exposure period of 8 hours. The decrease in AEC was maintained throughout the 8-h exposure period during oxidative phosphorylation and was inhibited; and recovery began after 2-h of removal of the inhibitor. The decrease in AEC due to inhibition of fatty acid oxidation reached a low after 2-h, after which recovery began, which is suggested to be due to activation of glycolysis to supply the oxidative substrates to mitochondria in place of fatty acids when β-oxidation is inhibited (Matsui, et al, 1994). Inhibition of glycolysis resulted in an irreversible decrease in AEC.

In the present study, decreases in intracellular ATP concentration, accompanied by increases in ADP, AMP and Pi concentrations, as well as decreases in AEC and PP during the accumulation and compound efflux phase of DOX-mediated P-gp transport were indicative of an increase in energy use associated with P-gp transport activity alone. It is believed that this is the first study to use AEC as an indicator of cellular energetic state associated with xenobiotic induced P-gp transport.

5.0 CONCLUSION

The evolution of cellular defense mechanisms as a means of dealing with endogenous and exogenous xenobiotics has enabled organisms to survive in chemically stressful environments. However recent work has suggested that through maintenance, regulation and activity these systems may impose significant energetic and metabolic costs on organisms which may ultimately lead to a decrease in the amount of energy available to processes like growth and reproduction and reduction in overall fitness.

This study functionally characterized the teleost drug efflux pump, P-gp and specifically examined the energetic costs associated with its transport activity. The results of this study suggest that there may be significant energetic costs associated with the active transport activity of P-gp as was evident from changes in adenylate parameters such as concentrations of ATP, ADP, and AMP as well as changes in AEC, and PP. Whether these costs are substantial in terms of an organisms overall energy budget, and ultimately their overall fitness remains a question to be answered. However, the energetic demand of P-gp and the associated costs are likely to increase during toxic challenge, and if combined with a situation where energy is limiting to an organism (e.g. winter exposure, low food availability), it is likely that these costs will be at the expense of other processes such as growth and reproduction, influence individual

performance and may translate into decreased fitness. In the case where the latter occurs there will be important implications for ecological and evolutionary processes.

LITERATURE CITED

Albertus, J. A., & Laine, R. O. (2001). Enhanced xenobiotic transporter expression in normal teleost hepatocytes: Response to environmental and chemotherapeutic toxins. *The Journal of experimental biology, 204*(2), 217-227.

Ambudkar, S. V., Dey, S., Hrycyna, C. A., Ramachandra, M., Pastan, I., & Gottesman, M. M. (1999). Biochemical, cellular, and pharmacological aspects of the multidrug transporter. *Annual Review of Pharmacology and Toxicology, 39*, 361-398.

Ambudkar, S.V., Cardarelli, C.O., Pashinsky, I. and Stein, W.D. (1997). Relation between the turnover number for vinblastine transport and for vinblastine-stimulated ATP hydrolysis by human P-glycoprotein. *J. Biol. Chem. 272*, 21160-21166.

Ataullakhanov, F. I., & Vitvitsky, V. M. (2002). What determines the intracellular ATP concentration. *Bioscience reports, 22*(5-6), 501-511.

Atkinson, D.E., (1971). Adenine nucleotides as stoichiometric coupling agents in metabolism and as regulatory modifiers: the adenylates energy charge. In: Vogel, H.J., (Eds.), *Metabolic regulation*. Academic Press Inc., New York, pp1-21.

Atkinson, D.E., (1977). Cellular energy metabolism and its regulation. Academic Press, New York.

Bains, O. S., & Kennedy, C. J. (2004). Energetic costs of pyrene metabolism in isolated hepatocytes of rainbow trout, *Oncorhynchus mykiss*. *Aquatic Toxicology, 67*(3), 217-226.

Bains, O. S., & Kennedy, C. J. (2005). Alterations in respiration rate of isolated rainbow trout hepatocytes exposed to the P-glycoprotein substrate rhodamine 123. *Toxicology, 214*(1-2), 87-98.

Baksi, S.M., Frazier. J.M. (1990). Isolated fish hepatocytes – model systems for toxicological research. *Aquatic Toxicology, 16*, 229-256.

Ball, W. J.,Jr, & Atkinson, D. E. (1975). Adenylate energy charge in saccharomyces cerevisiae during starvation. *Journal of Bacteriology, 121*(3), 975-982.

Ballet, F., Vrignaud, P., Robert, J., Rey, C., Poupon, R. (1987). Hepatic extraction, metabolism and biliary excretion of doxorubicin in the isolated perfused rat liver. *Cancer Chemother. Pharmacol., 19*, 240-245.

Bard S.M., Bello S.M., Hahn M.E., Stegeman J.J. 2002. Expression of P-glycoprotein in killifish (*Fundulus heteroclitus*) exposed to environmental xenobiotics. *Aquatuc Toxicol. 59(3)*, 237-251.

Bard, S. M. (2000). Multixenobiotic resistance as a cellular defense mechanism in aquatic organisms. *Aquatic Toxicol. 48*(4), 357-389.

Behm, C. A., & Bryant, C. (1975). Studies of regulatory metabolism in moniezia expansa: General considerations. *International journal for parasitology, 5*(2), 209-217.

Berticat, C., Boquien, G., Raymond, M., Chevillon, C., (2002). Insecticide resistance genes induce a mating competition cost in *Culex pipiens* mosquitoes. *Genet. Res., 79*, 41-47.

Berticat, C., Duron, O., Heyse, D., Raymond, M., (2004). Insecticide resistance genes confer a predation cost on mosquitoes, *Culex pipiens. Genet. Res., 83*, 189-196.

Bogdanova, A., Grenacher, B., Nikinmaa, M., Gassmann, M., (2005). Hypoxic responses of Na^+/K^+ ATPase in trout hepatocytes. *J. Exp. Biol., 208*, 1793-1801.

Boivin, T., Chabert-d'Hières, C., Bouvier, J.C., Beslay, D., Sauphaor, B., (2001). Pleiotropy of insecticide resistance in the codling moth, *Cydia pmonella. Ent. Exp. Appl., 99*, 381-386.

Booth, C.I., Brouwer, K.R., Brouwer, K.L. (1998). Effect of multidrug resistance modulators on the hepatobiliary disposition of doxorubicin in the isolated perfused rat liver. *Cancer Res., 58*, 3641-3648.

Borst, P., Evers, R., Kool, M., & Wijnholds, J. (2000). A family of drug transporters: The multidrug resistance-associated proteins. *Journal of the National Cancer Institute, 92*(16), 1295-1302.

Brett, J.R., Groves, D.D. (1979). Physiological energetics. In: Hoar, W.S., Randall, D.R., Brett, J.R. (Eds.) *Fish Physiology: Bioenergetics and Growth*, vol 8. Academic Press, New York, pp 279-352.

Calderwood, S. K., Bump, E. A., Stevenson, M. A., Van Kersen, I., & Hahn, G. M. (1985). Investigation of adenylate energy charge, phosphorylation potential, and ATP concentration in cells stressed with starvation and heat. *Journal of cellular physiology, 124*(2), 261-268.

Callaghan, R., Ford, R.C., Kerr, I.D. (2006). Minireview: the translocation mechanism of p-glycoprotein. *FEBS Letters. 580*, 1056-1063.

Casey, C.A, Perlman, D.F., Vorhaben, J.E., Campbell, N.W. (1983). Hepatic ammoniagenesis in the channel catfish, *Ictalurus punctuatus. Mol. Physiol. 3*, 107-126.

Chan, K., Davies, P., Childs, S., Veinot, L., & Ling, V. (1992). P-glycoprotein genes in the winter flounder, pleuronectes americanus: Isolation of two types of genomic clones carrying 3′ terminal exons. *Biochimica et Biophysica Acta (BBA) - Gene Structure and Expression, 1171*(1), 65-72.

Chapman, A. G., Fall, L., & Atkinson, D. E. (1971). Adenylate energy charge in escherichia coli during growth and starvation. *Journal of Bacteriology, 108*(3), 1072-1086.

Chapman, A.G., Atkinson, D.E. (1973). Stabilization of the adenylate energy charge by the adenylates deaminase reaction. *J. Biol. Chem. 24(8)*, 8309-8312.

Childs, S., Yeh, R. L., Georges, E., & Ling, V. (1995). Identification of a sister gene to P-glycoprotein. *Cancer research, 55*(10), 2029-2034.

Cogan, E.B. (1999). A robotics-based automated assay for inorganic and organic phosphates. *Anal Biochem.* 271(1):29-35.

Cooper, P.S., 1996. Expression of the xenobiotic transport P-glycoprotein in the mummichog (*Fundulus heteroclitus*). PhD thesis. School of Marine Science, College of William and Mary, Williamsburg, VA.

Cornwall, R., Toomey, B. H., Bard, S., Bacon, C., Jarman, W. M., & Epel, D. (1995). Characterization of multixenobiotic/multidrug transport in the gills of the mussel mytilus californianus and identification of environmental substrates. *Aquatic Toxicology, 31*(4), 277-296.

Cree I.A. and Andreotti P.E. (1997). Measurement of cytotoxicity by ATP - based luminescence assay in primary cell cultures and cell lines. *Toxicology in Vitro, 11*, 553 – 556.

Cresswell, J.E., Merritt, S.Z., Martin, M.M., (1992). The effect of dietary nicotine on the allocation of assimilated food to energy metabolism and growth in fourth-instar larvae of the southern army worm *Spodoptera-eridania* Lepidoptera Noctuidae. *Oncologia*, *89*(3), 449–453.

Croop, J. M. (1993). P-glycoprotein structure and evolutionary homologies. *Cytotechnology, 12*(1-3), 1-32.

Crouch S.P.M., Kozlowski R., Slater K.J. and Fletcher J. (1993). The use of ATP bioluminescence as a measure of cell proliferation and cytotoxicity. *J. Immunol. Methods, 160*, 81 – 88.

Cullinane, C., Cutts, S.M., van Rosmalen, A., Phillips, D.R., (1994). Formation of adriamycin-DNA adducts in vitro. *Nucleic Acids Res. 22*, 2296-2303.

Danø, K. (1973). Active outward transport of daunomycin in resistant ehrlich ascites tumor cells. *Biochimica et biophysica acta, 323*(3), 466-483.

Dash, J.A., (1988). Effect of dietary terpenes on glucoronic acid excretion and ascorbic acid turnover in the brushtail possum (*Trichorsurus vulpecula*). *Comp. Biochem. Physiol. 89B*, 221-226.

Driedzic, W.R., Hochachka, P.W. (1976). Control of energy metabolism in fish white muscle. *Am. J. Physiol. 230*, 579-582.

Ekman P., Jager, O. (1993). Quantification of subnanomolar amounts of phosphate bound to seryl and threonyl residues in phosphoproteins using alkaline hydrolysis and malachite green. *Anal Biochem.* 214(1):138-141.

Endicott, J. A., & Ling, V. (1989). The biochemistry of P-glycoprotein-mediated multidrug resistance. *Annual Review of Biochemistry, 58*, 137-171.

Epel, D. (1998). Use of multidrug transporters as first lines of defense against toxins in aquatic organisms. *Comparative Biochemistry and Physiology - Part A: Molecular & Integrative Physiology, 120*(1), 23-28.

Eytan, G. D., & Kuchel, P. W. (1999). Mechanism of action of P-glycoprotein in relation to passive membrane permeation. *International review of cytology, 190*, 175-250.

Eytan, G.D., Regev, R. and Assaraf, Y.G. (1996). Functional reconstitution of P-glycoprotein reveals an apparent near stoichiometric drug transport to ATP hydrolysis. *J. Biol. Chem. 271*, 3172–3178.

Fedorow, C. A., Churchill, T. A., & Kneteman, N. M. (1998). Effects of hypothermic hypoxia on anaerobic energy metabolism in isolated anuran livers. *Journal of comparative physiology.B, Biochemical, systemic, and environmental physiology, 168*(8), 555-561.

Finne, E.F., Cooper, G.A.., Koop, B.F., Hylland, K., Tollefsen, K.E. (2007). Toxicogenomic responses in rainbow trout (*Oncorhynchus mykiss*) hepatocytes exposed to model chemicals and a synthetic mixture. *Aquat. Toxicol. 81(3)*, 293-303.

Fisher, D. K., Higgins, T.J. (1994). A sensitive, high-volume, colorimetric assay for protein phosphatases. *Pharm Res.* 11:759-763.

Foley,W.J., (1992). Nitrogen and energy retention and acid–base status in the common ringtail possum, *Pseudocheirus peregrinus*, evidence of the effects of absorbed allelochemicals. *Physiol. Zool. 65* (2), 403–421.

Foley, W.J., McLean, S., Cork, S.J .(1995) Consequences of biotransformation of plant secondary metabolites on acid-base metabolism in mammals – a final common pathway? *Journal of Chemical Ecology 21*, 721–774.

Foster, S.P. Woodcock, C.M., Williamson, M.S., Devonshire, A.L, Dennholm, I., Thomson, R., (1999). Reduced alarm response by peach-potato aphids, *Myzus persicae* (Hemiptera:Aphidiae), with knock-down resistance to insecticides (kdr) may impose a fitness cost through increased vulnerability to natural enemies. *Bull. Entomol. Res. 89*, 133-138.

Gagné, F, Blaise, C. 1999. Toxicological Effects of Municipal Wastewaters to Rainbow Trout Hepatocytes. *Bull. Environ. Contam. Toxicol. 63*(4), 503-510.

Galgani, F., Cornwall, R., Holland Toomey, B., & Epel, D. D. (1996). Interaction of environmental xenobiotics with a multixenobiotic defense mechanisms in the bay mussel *Mytilus galloprovincialis* from the coast of California. *Environmental Toxicology and Chemistry, 15*(3), 325-331.

Gallois, L., Fiallo, M., Barnier-Suillerot, A. (1998). Comparison of the interaction of doxorubicin, daunorubicin, idarubicin and idarubicinol with large unilamellar vesicles cirucular dichroism study. *Biochemica et Biophysica Acta 1370(1)*, 31-40.

Germann, U.A. (1996). P-glycoprotein – a mediator of multidrug resistance in tumour cells. *Eur. J. Cancer 32A*, 927-944.

Gewirtz, D.A., 1999. A Critical evaluation of the mechanisms of action proposed for the antitumor effects of the anthracycline antibiotics adriamycin and daunorubicin. *Biochem. Pharmacol. 57*, 727- 741.

Gill, K.A., Walsh, P.J., (1990). Effects of temperature on metabolism of benzo[a]pyrene by toadfish (*Opsanus beta*) hepatocytes. *Can. J. Fish. Aquat. Sci. 47*, 831-837.

Glick, Z., Joselyn, M. A. (1970*b*). Effect of tannic acid and related compounds on the absorption and utilization of proteins in the rat. *J. Nutrition. 100*, 516-520.

Glick, Z., Joselyn, M.A. (1970*a*). Food intake depression and other metabolic effects of tannic acid in the rat. *J. Nutrition 100,* 509-515.

Gorman, M.W., Marble, D.R., Ogimoto, K., Feigi, E.O. (2003). Measurement of adenine nucleotides in plasma. *Luminescence 18*, 173-181.

Gottesman M.M, Pastan I. (1993). Biochemistry of multidrug resistance mediated by the multidrug transporter. *Annu. Rev. Biochem.62*, 385–427.

Gottesman, M. M., & Pastan, I. (1988). The multidrug transporter, a double-edged sword. *The Journal of biological chemistry, 263*(25), 12163-12166.

Guglielmo, C.G., Karasov, W.H., Jukubas, W.J. (1996). Nutritional costs of a plan secondary metabolite explain selective foraging by ruffed grouse. *Ecol. 77*(4), 1103-1115.

Hassinen, I. E., & Hiltunen, K. (1975). Respiratory control in isolated perfused rat heart. role of the equilibrium relations between the mitochondrial electron carriers and the adenylate system. *Biochimica et biophysica acta, 408*(3), 319-330.

Hazel, J.R. (1982). The incorporation of unsaturated fatty acids of the n-9, n-6, and n-3 families into individual phospholipids by isolated hepatocytes of thermally-acclimated rainbow trout, *Salmo gairderi. J. Exp. Zool. 167*, 167-176.

Heath, A.G. (1984). Changes in tissue adenylates and water content of bluegill, *Lepomis macrochirus*, exposed to copper. *J. Fish Biol. 24*, 299-309.

Hemmer, M. J., Courtney, L. A., & Ortego, L. S. (1995). Immunohistochemical detection of P-glycoprotein in teleost tissues using mammalian polyclonal and monoclonal antibodies. *The Journal of experimental zoology, 272*(1), 69-77.

Hennessy, M., & Spiers, J. P. (2007). A primer on the mechanics of P-glycoprotein the multidrug transporter. *Pharmacological research : the official journal of the Italian Pharmacological Society, 55*(1), 1-15.

Higgins., C.F., (1992). ABC transporters: from microorganisms to man. *Ann. Rev. Cell. Biol. 8*, 67-113.

Hilmer, S.N., Cogger, V.C., Muller, M., LeCouteur, D.G. (2004). The hepatic pharmacokinetics of doxorubicin and lipsomal doxorubicin. *Drug Metab Dispos. 32*: 794-799.

Jedlitschky, G., Leier, I., Buchholz, U., Center, M., & Keppler, D. (1994). ATP-dependent transport of glutathione S-conjugates by the multidrug resistance-associated protein. *Cancer research, 54*(18), 4833-4836.

Kangas L., Grönroos M. and Nieminen A.L. (1984). Bioluminescence of cellular ATP: a new method for evaluating agents in vitro. *Medical Biology, 62*, 338 – 343.

Kitchell, J.F., 1983. Energetics. In Webb, P.W., Weihs, D. (Eds.) *Fish Biomechanics*. Praeger Publishers, New York, pp. 312-338.

Klaunig, J.E., (1994). Establishment of fish hepatocyte cultures for use in in vitro carcinogenicity studies. *Natl. Cancer Inst. Monogr., 65*, 163-73.

Klaassen, C.D., Watkins, J.B. (1999). Casarett & Doull's toxicology: the basic science of poisons (5^{th} Eds.) McGraw-Hill Companies Inc., New York.

Kleinow, K. M., Doi, A. M., & Smith, A. A. (2000). Distribution and inducibility of P-glycoprotein in the catfish: Immunohistochemical detection using the mammalian C-219 monoclonal. *Marine environmental research, 50*(1-5), 313-317.

Koban, M., Graham, G. Prosser, C. L. (1987). Induction of heat shock protein synthesis in teleost hepatocytes: effects of acclimation temperature. *Physiol. Zool.* 60, 290–296.

Kohane, M. J., & Watt, W. B. (1999). Flight-muscle adenylate pool responses to flight demands and thermal constraints in individual colias eurytheme (lepidoptera, pieridae). *The Journal of experimental biology, 202*(Pt 22), 3145-3154.

Kurelec, B. (1992). The multixenobiotic resistance mechanism in aquatic organisms. *Critical reviews in toxicology, 22*(1), 23-43.

Kurelec, B., & Pivcevic, B. (1989). Distinct glutathione-dependent enzyme activities and a verapamil-sensitive binding of xenobiotics in a fresh-water mussel anodonta cygnea. *Biochemical and biophysical research communications, 164*(2), 934-940.

Kurelec, B., Pivcevic, B., (1991). Evidence for a multixenobiotic resistance mechanism in the mussel *Mytilus galloprovincialis. Aquat. Toxicol. 19*, 291-302.

Lefrak, E.A., Pitha J., Rosenheim, S. & Gottlieb, J.A. (1973). A clinical pathological analysis of adriamycin cardiotoxicity. *Cancer*, 32: 302-314.

LeBras, S. (1995) Adenosine Energy Charge (AEC) for *Asellus Aquaticus L.* (Crustacea, Isopoda) after Lindane Contamination during a Period of 48 h. *Rev. Sci. Eau 8*(4), 493-503.

Lehinger, A.L. (2005). *Principles of Biochemistry (4th Eds.)*, W.H. Freeman and Company, New York.

Lehinger, A.L., (1975). *Biochemistry*, Worth Publishers, Inc., New York.

Lehninger, A.L. (1965). *Bioenergetics*, Menlo Park, CA: W.A. Benjamin.

Li, Q., Yu, W.F., Zhou, M.T., Lu, X., Yang, L.Q., Song, J.G., Lu, J.H. (2005). Isoflurane preserves energy balance in isolated hepatocytes during *in vitro* anoxia/reoxygenation. *World J. Gastroenterol. 11*(25), 3920-2924.

Litman, T., Druley, T. E., Stein, W. D., & Bates, S. E. (2001). From MDR to MXR: New understanding of multidrug resistance systems, their properties and clinical significance. *Cellular and molecular life sciences 58*(7), 931-959.

Lundin A., Hasenson M., Persson J. and Pousette A. (1986). Estimation of biomass in growing cell lines by ATP assay. *Methods Enzymol.133*, 27 – 42 3.

MacFarlane, R.B. (1981). Alterations in adenine nucleotide metabolism in the Gulf Killifish (*Fundulus grandis*) induced by low pH water. *Comp. Biochem. Physiol. 66B*, 193-202.

Malins, D.C., Ostrander, G.K. (1991). Perspectives in aquatic toxicology. Annu. *Rev. Pharmacol. Toxicol., 31*, 371-399.

Marazza, D.J., Bornens, P.H., Le Gal, Y. Effects of ammonia on survival and adenylates energy charge in the shrimp Palaemonetes varians. *Ecotoxicol. Environ. Safety, 34*, 103-108.

Marchanda J., Quiniou L., Riso R., Thebault, M.T., Laroche J. (2004). Physiological cost of tolerence to toxicants in the European flounder *Platichtys flexus* along the French Atlantic coast. *Aquat Toxicol, I(4)*, 20 décember 2004, pages 327-343.

Martin, C., Berridge, G., Mistry, P., Higgins, C., Charlton, P., & Callaghan, R. (1999). The molecular interaction of the high affinity reversal agent XR9576 with P-glycoprotein. *British journal of pharmacology, 128*(2), 403-411.

Maryanski, M., Kramarz, P., Laskowski, R., Niklinska, M., (2002). Decreased energetic reserves, morphological changes and accumulation of metals in carabid beetles (*Poecilus cupreus* L.) exposed to zinc- or cadmium-contaminated food. *Ecotox. 11,* 127-139.

Matsui Y., Kitade H., Kamiya T., Kanemaki T., Hiramatsu Y., Okumura T., Kamiyama Y. 1994. Adenylate energy charge of rat and human cultured hepatocytes. *In Vitro Cell Dev Biol Anim. 30A(9)*, 609-14.

Mckenzie, J.A., Batterham, P. (1994). The genetic, molecular and phenotypic consequences of selection for insecticide resistance. *Trends. Ecol. Evol. 9*, 227-237.

Migula, P., Geowacka, E., Nuorteva, S.L., Nuroteva, P., Tulisalo, E. (1997). Time-related effects of intoxication with cadmium and mercury in the red wood ant. *Ecotox. 6*, 307-320.

Minier, C., Moore, M.N., (1996). Rhodamine B accumulation and MXR protein expression in mussel blood cells: effects of exposure to vincristine. *Mar. Ecol. Prog. Ser. 142*, 165-173.

Mistry, P., Alistair, J.S., Dangerfield, W., Okiji, S., Liddle, C., Bootle, C., Plumb, A., Templeton, D., Charlton, P. (2001). *In vitro* and *in vivo* reversal of P-glycoprotein-mediated multidrug resistance by a novel potent modulator, XR9576. *Cancer Res. 61*, 749-758.

Mommsen, T.P., Lazier, C.B. (1986). Stimulation of estrogen receptor accumulation by estradiol in primary cultures of salmon hepatocytes. FEBS Letters, 195, 269-271.

Montague, M. D., & Dawes, E. A. (1974). The survival of peptococcus prevotii in relation to the adenylate energy charge. *Journal of general microbiology, 80*(1), 291-299.

Moon, T.W., Walsh, P.J., Mommsen, T.P., (1985). Fish hepatocytes: A model metabolic system. Can. J. Fish. Aquat. Sci. 42(11), 1772-1782.

Nicholson, R.A., (1994). Excitatory actions of dehydroabietic acid on mammalian synaptosomes. *Pharmacol. Toxicol. 75(5)*, 274-279.

Nilsson, L., Kogure, K., & Busto, R. (1975). Effects of hypothermia and hyperthermia on brain energy metabolism. *Acta Anaesthesiologica Scandinavica. 19*(3), 199-205.

Olson R.D. & Mushlin, P.S. (1990). Doxorubicin cardiotoxicity: ananlysis of prevailing hypotheses. *FASEB Journal, 4*, 3076-3086.

Olson, R.D., Mushlin, P.S., Brenner, D.E., Fleischer, S., Cusack, B.J., Chang, B.K., Boucek, R.J., 1988. Doxorubicin cardiotoxicity may be caused by its metabolite, doxorubicinol. *Proc. Natl. Acad. Sci. USA 85*, 3585-3589.

Overgaard, J., Gesser, H. (2004). Force development, energy state and ATP production of cardiac muscle from turtles and trout during normoxia and severe hypoxia. *Journal of Experimental Biology. 207*, 1915-1924

Pesonen, M., Anderson, T., (1992). Toxic effects of bleached and unbleached paper mill effluents in primary cultures of rainbow trout hepatocytes. *Ecotoxicol. Environ. Saf. 24*, 63-71.

Petty R.D., Sutherland L.A., Hunter E.M. and Cree I.A. (1995). Comparison of MTT and ATP – based assays for the measurement of viable cell number. J. *Biolumin. Chemilumin.10*, 29 – 34.

Picado, A. M., and Le Gal, Y. (1990). Assessment of industrial sewage impacts by adenylate energy charge measurements in the bivalve *Cerastoderma edule. Ecotoxicol. Environ. Safety. 19*, 1–7.

Pradet A, Raymond P., (1983). Adenine nucleotide ratios and adenylate energy charge in energy metabolism. *Annu. Rev. Plant Physiol. 34*,199–224.

Ridge, J. W. (1972). Hypoxia and the energy charge of the cerebral adenylate pool. *The Biochemical journal, 127*(2), 351-355.

Risso-de Faverney, C., Devaus, A., Girard, J.P., BAily, B., Rahmani, R. 2002. Cadmium induces apoptosis and genotoxicity in rainbow trout hepatocytes through generation of reactive oxygen species. *Aquat. Toxicol. 53(1)*, 65-76.

Roe, M., Folkes, A., Ashworth, P., Brumwell, J., Chima, L., Hunjan, S., et al. (1999). Reversal of P-glycoprotein mediated multidrug resistance by novel anthranilamide derivatives. *Bioorganic & medicinal chemistry letters, 9*(4), 595-600.

Shapiro, A.B. and Ling, V. (1998). Stoichiometry of coupling of rhodamine 123 transport to ATP hydrolysis by P-glycoprotein. *Eur. J. Biochem. 254*, 189–193.

Sharom, F. J., Yu, X., Chu, J. W., & Doige, C. A. (1995). Characterization of the ATPase activity of P-glycoprotein from multidrug-resistant chinese hamster ovary cells. *The Biochemical journal, 308* (2), 381-390.

Shofer, S.L., Tjeerdema, R.S. (1998). Effects of hypoxia and toxicant exposure on adenylates energy charge and cytosolic ADP concentrations in abalone. *Comp. Biochem. Physiol. 119C*,(1), 51-57.

Siebert, H., (1985). Viability control and oxygen consumption of isolated hepatocytes from thermally acclimated rainbow trout (*Salmo gairdnerii*). *Comp. Biochem. Physiol. 80B*(4), 677-683.

Singal PK, Deally C.M.R., Weinberg, L.E., (1987). Subcellular effects of adryamicin in the heart: a concise review. *Journal of Molecular and Cellular Cardiology, 19*, 817-828.

Singal, P.K., Li, T., Kumar, D., Danelisen, I., Iliskovic, N., (2000). Adriamycin-induced heart-failure: mechanism and modulation. *Mol. Cell. Biochem. 207*, 77-85.

Simon, E., (1985). Subcellular distribution of ATP and ADP in isolated hepatocytes of rainbow trout. Comp. Biochem. Physiol., 80B, 573-576.

Slater EC (1979) Measurement and importance of phosphorylation potentials: calculation of the free energy of hydrolysis in cells. In: Fleischer S, Packer L (Eds.), *Methods in enzymology*, vol 55. Academic Press, New York, pp 235-245.

Stegman, J.J., Hahn, M.E. (1993). Biochemistry and molecular biology of monoxygenases: current perspectives on forms, functions, and regulation of cytochrome P450 in aquatic species. In: Malins, D.C., Ostrander, G.K. (Eds.) *Aquatic Toxicology*: *molecular, biochemical, and cellular perspectives.* CRC Press, Inc, Florida, pp 87-206.

Stewart, A.J., Mistry, P., Dangerfield, W., Okiji, S. and Templeton, D. 1998. XR9576, a potent modulator of P-glycoprotein mediated resistance. Annals. of Oncology, 9, Abstract 556.

Storer R.D., McKelvey T.W., Kraynak A.R., Elia M.C., Barnum J.E., Harmon L.S., Nichols W.W. and Deluca J.G. (1996). Revalidation of the in vitro alkaline elution/rat hepatocyte assay for DNA damage: improved criteria for assessment of cytotoxicity and genotoxicity and the results for 81 compounds. *Mutation Research, 368*, 59 – 101.

Sturm, A., Ziemann, C., Hirsch-Ernst, K.I., Segner, H., 2001. Expression and functional activity of P-glycoprotein in cultured hepatocytes from *Oncorhynchus mykiss*. *Am. J. Physiol. Regul. Integr. Comp. Physiol. 281*, 1119–1126.

Tanaka, M., andYoshida, S., 1980. Mechanism of the inhibition of calf thymus DNA polymerases a and b by daunomycin and adriamycin. *J. Biochem. 87*, 911-918.

van Veen, H.W. and Callaghan, R. (2003). In: ABC Proteins: From Bacteria to Man (Holland, I.B., Cole, S.P.C., Kuchler, K., Higgins, C.F., Eds.), pp. 81–106, Elsevier, London.

Wacher VJ, Wu C-Y and Benet LZ (1995) Overlapping substrate specificities and tissue distribution of cytochrome P450 3A and P-glycoprotein: Implications for drug delivery and activity in cancer chemotherapy. *Mol Carcinog* **13:** 129-134

Walesby, N.J., Johnston, I.A. (1980). Temperature acclimation in brook trout muscle: Adenine nucleotide concentrations, phosphorylation state, and adenylates energy charge. *J. Comp. Physiol. 139A*, 127-133.

Walker, J., Martin, C., Callaghan, R., (2004). Inhibition of Pglycoprotein function by XR9576 in a solid tumour model can restore anticancer drug efficacy. *Eur. J. Cancer 40*, 594–605.

Walsh, P.J., Foster, G., Moon, T.W. (1983). The effects of temperature on metabolism of the American eel, *Anguilla rostrata* (LeSueur): compensation in the summer and torpor in the winter. *Physiol. Zool. 56*, 532-540.

Wieser, W., Medgyesy, N. (1990). Aerobic maximum for growth in the larvae and juveniles of a cyprinid fish, *Rutilus rutilus* (L.): implications for energy budgeting in small poikilotherms. *Funct. Ecol. 4*(2), 233–242.

Wilson, D. F., Stubbs, M., Veech, R. L., Erecinska, M., & Krebs, H. A. (1974a). Equilibrium relations between the oxidation-reduction reactions and the adenosine triphosphate synthesis in suspensions of isolated liver cells. *The Biochemical journal, 140*(1), 57-64.

Wilson, D.F., Stubbs, M., Oshino, M., Erecinska, M. (1974b). Thermodynamic relationships between the mitochondrial oxidation-reduction reactions and cellular ATP levels in ascites tumor cells and perfused rat liver. *Biochemistry 13*, 5305-5311.

Xie, X.J., Sun. R., (1993). Pattern of energy allocation in the southern catfish (Silurus meridonalis). *J. Fish Biol. 42*(2), 197-207.

Zaroogian., G.E., Johnson., M., (1989). Adenylate energy charge and adenine nucleotide measurements as indicators of stress in the mussel, *Mytilus edulis*, treated with dredged material under laboratory conditions. *Bull. Environ. Contam. Toxicol. 43*, 428-435.